

REPORT DOCUMENTATION PAGE				Form Approved OMB No. 0704-0188	
The public reporting burden for this collection of information is estimated to average 1 hour per response, including the time for reviewing instructions, searching existing data sources, gathering and maintaining the data needed, and completing and reviewing the collection of information. Send comments regarding this burden estimate or any other aspect of this collection of information, including suggestions for reducing the burden, to the Department of Defense, Executive Services and Communications Directorate (0704-0188). Respondents should be aware that notwithstanding any other provision of law, no person shall be subject to any penalty for failing to comply with a collection of information if it does not display a currently valid OMB control number.					
PLEASE DO NOT RETURN YOUR FORM TO THE ABOVE ORGANIZATION.					
1. REPORT DATE (DD-MM-YYYY) 03-10-2007		2. REPORT TYPE Final		3. DATES COVERED (From - To) 02/15/2005 - 03/31/2007	
4. TITLE AND SUBTITLE Multifunctional Oxide Films for Advanced Multifunction RF Systems, Phase III				5a. CONTRACT NUMBER	
				5b. GRANT NUMBER N00014-05-1-0238	
				5c. PROGRAM ELEMENT NUMBER	
6. AUTHOR(S) Dr. Volker D. Heydemann				5d. PROJECT NUMBER	
				5e. TASK NUMBER	
				5f. WORK UNIT NUMBER	
7. PERFORMING ORGANIZATION NAME(S) AND ADDRESS(ES) Penn State Electro-Optics Center 222 Northpointe Blvd. Freeport, PA 16229				8. PERFORMING ORGANIZATION REPORT NUMBER	
9. SPONSORING/MONITORING AGENCY NAME(S) AND ADDRESS(ES) OFFICE OF NAVAL RESEARCH REGIONAL OFFICE CHICAGO 230 SOUTH DEARBORN, ROOM 380 CHICAGO IL 60604-1595 Fax: (312) -886-2094				10. SPONSOR/MONITOR'S ACRONYM(S)	
				11. SPONSOR/MONITOR'S REPORT NUMBER(S)	
DISTRIBUTION STATEMENT A Approved for Public Release Distribution Unlimited					
13. SUPPLEMENTARY NOTES					
14. ABSTRACT The Electro-Optics Center of the Pennsylvania State University procured and established a custom-designed molecular beam epitaxy (MBE) system and commenced growth of oxide (TiO ₂ , STO, BTO, BST and MgO) and III-nitride (AlN, GaN) thin films. The growth parameters and layer properties of these films were investigated by various in-situ and ex-situ characterization techniques under the aspect of developing a AlGa _N HEMT epitaxy process, a BST varactor epitaxy process and aiding the integration of BST epitaxy on III-nitride templates using MgO buffer layers. Methods for the dielectric characterization of the epitaxial oxide films have been evaluated and applied in collaboration with Dr. Lanagan (Penn State Materials Research Laboratory).					
15. SUBJECT TERMS Multifunctional Oxides, BST varactors, barium strontium titanate, oxide / nitride integration, thin film growth, molecular beam epitaxy, dielectric characterization, oxide stoichiometry control, BST stoichiometry control					
16. SECURITY CLASSIFICATION OF:			17. LIMITATION OF ABSTRACT	18. NUMBER OF PAGES	19a. NAME OF RESPONSIBLE PERSON Colin Wood, woodc@onr.navy.mil
a. REPORT Unclassified	b. ABSTRACT Unclassified	c. THIS PAGE Unclassified			19b. TELEPHONE NUMBER (Include area code) (703) 696-4218

PENNSTATE



Electro-Optics Center

Final Report for

ONR Grant N00014-05-1-0238

Multifunctional Oxide Films for Advanced Multifunction RF Systems Phase III

Reporting period 15 Feb 2005 – 31 Mar 2007

Compiled by Dr. Volker D. Heydemann (Research Associate)
Penn State Electro-Optics Center
559-A Freeport Road
Freeport PA 16229
Phone 724-295-6605
Fax: 724-295-6617
E-mail: vheydemann@eoc.psu.edu

Date 14 September 2007

Submitted to Dr. Colin Wood
Electronics Division - Code 312
Office of Naval Research
875 North Randolph St,
Arlington, VA 22203-1995
Phone 703-696-4218
Fax: 703-696-2611
E-mail: woodce@onr.navy.mil

20071015471

Abstract

During the reporting period, the Electro-Optics Center of the Pennsylvania State University procured and established a custom-designed molecular beam epitaxy (MBE) system and commenced growth of oxide and nitride thin films. The films were characterized, as applicable, by *in-situ* reflected high energy electron diffraction (RHEED), flux monitoring, residual gas analysis, and multi-beam optical stress sensor (MOSS) analysis (III-nitrides only) as well as *ex-situ* atomic force microscopy (AFM), x-ray rocking curves and high resolution x-ray diffraction (HRXRD), Rutherford backscattering (RBS), cross-section transmission electron microscopy and diffraction (XTEM), and RF loss metrology.

High quality TiO_2 epitaxial layers produced by sputter deposition at Penn State DMSE and by MBE at Penn State EOC were used by Lance Haney, PSU graduate student, to investigate the applicability of various RF metrology methods for the determination of the layers' dielectric properties, losses and – for future BST films – tunability. Mr. Haney graduated during the reporting period. A split-cavity metrology system has been set up at PSU EOC, in close collaboration with Dr. Mike Lanagan (PSU Materials Research Lab), to allow for quick turnaround in-house layer evaluation.

A study of stable Sr/Ti ratios in MBE-grown $\text{Sr}_x\text{Ti}_y\text{O}_z$ has been conducted by Patrick Fisher, CMU graduate student utilizing EOC's MBE system, as part of his PhD thesis work.

Stoichiometry control was identified as a crucial issue during the TiO_2 and STO growth experiments and the initial BST growth runs. HRXRD and Rutherford backscattering were used to determine the composition and layer stoichiometry. Inherently, both these methods feature a resolution of approximately 1%, thus RHEED-induced EDX ("RHEED TRAXS") to the oxide MBE is being investigated as a potential method to determine the layer stoichiometry and composition more precisely *in-situ*.

Graduate student Matthew Snyder established an MBE growth process for high quality MgO epitaxial layers that will be used for the integration of tunable oxides on SiC and III-nitride substrates or templates. A study of the impact of MgO / substrate lattice mismatch has been conducted indicating that single crystal MgO films can be deposited on substrates with less than 8% lattice mismatch.

BACKGROUND

The US Navy faces multiple challenges in the 21st century following the changing nature of its mission and technological advances worldwide. The general objective of these changes is gaining information superiority and total situational awareness. This requires new capabilities of detection and communication systems. Until recently, separate RF systems were implemented for radar, communication, and electronic warfare functions. Such architectures pose inherent limitations such as difficulty in tracking stealth targets, lack of interoperability between platforms, interference between systems, and high radar cross-section.

The new approach to these challenges is the integration of radar, communication, and EW capabilities using multifunction RF systems. New materials and device technologies need to be developed the next generation of multifunction RF systems. The system performance requirements are driving the development of new materials, such as wide bandgap semiconductor materials, and novel device structures that are essential for high power amplifiers at or beyond X-band frequencies. The improvements of active device performance need to be complemented by adequate improvements of passive components. Specifically, an emerging need for tunable capacitors with wide tunability range and capability of operation at high power levels nurtures the development of novel passive components and suitable high performance materials. Possible approaches to this particular application include micro-electro-mechanical systems and semiconductor-based varistors. The most promising approach, however, is the development of capacitors based on high-k dielectric materials. Many high-k materials systems have been investigated, and several, including $\text{Ba}_{1-x}\text{Sr}_x\text{TiO}_3$ [1-6], SrTiO_3 [2,3] and $\text{Na}_{0.5}\text{K}_{0.5}\text{NbO}_3$ [4] show considerable promise for the application in tunable, high power capacitors.

The implementation of novel dielectric materials in next generation RF systems depends on specific materials technology improvements. A prevalent problem to be addressed in the development of tunable capacitors are inherent dielectric losses which are currently at least an order of magnitude too high. According to literature accounts, the best paraelectric films exhibit loss tangent values of $10^{-1} - 10^{-2}$. In order to implement such materials for tunable capacitor applications, the loss tangent needs to be reduced to 10^{-3} or lower. Additionally, the tunability range of such materials needs to be extended by improvements to the material quality to reduce premature breakdown induced by poor material quality.

TECHNICAL CHALLENGES

In order to successfully incorporate crystalline oxide films into high frequency device structures, a number of technical challenges need to be resolved:

Improvement of film quality:

Most techniques used for the deposition of oxide thin films (such as laser ablation, sputtering, and sol-gel processes followed by firing) result in films with high defect density. Typical x-ray reflection peak widths of such films are in the 0.1 – 1 degree range indicating the oriented polycrystalline structure of the films. Commonly, such films exhibit high porosity, inclusions of secondary condensed phases, grain boundaries, dislocations, and high strain areas. Inclusions of ferroelectric phases in a paraelectric matrix are likely cause for increased dielectric losses.

Control of layer stoichiometry:

Oxides exhibit high densities of vacancy-type defects. This is known to lead to ferroelectric fatigue, degradation of the remnant field, and, in some cases, to the formation of secondary phases.

Control of the semiconductor / oxide interface:

Most oxides are not thermodynamically stable when they contact semiconductor surfaces, which leads to the formation of an interfacial amorphous oxide either during growth or subsequent processing. The oxide / semiconductor interface frequently exhibits a high density of interface states. Both effects are detrimental for device applications of such oxide layers targeting to induce high channel carrier density or for capacitors.

Identification of optimal substrate / ferroelectric / metal electrode combination.

The nascent technology of high-k dielectric materials for tunable filters to date still lacks a broad knowledge base of basic materials properties and effects of interface interaction of multiple materials that are used in tunable filter devices. In particular, material interactions and interface effects of tunable filter structures deposited on the semiconductor substrates as part of the MMIC circuits are widely unexplored. Most issues such as a lattice mismatch, strain relaxation, interface stability, suitable deposition regimes have to date not been addressed. As the initial data on simple material systems and devices become available, it will be necessary to reevaluate the material selections and propose a second iteration approach to identified problems in order to achieve the device performance targets enabling the use of tunable oxide capacitors in next generation RF systems.

CURRENT PROJECT STATUS

The major thrusts for the project during the reporting period were:

1. Setup and verification of the molecular beam epitaxy (MBE) system
2. Setup of a dedicated MBE sample preparation laboratory / cleanroom
3. Installation and verification of the multi-beam optical stress sensor (MOSS) system
4. Growth and characterization of III-nitride thin films
5. Growth and characterization of oxide thin films
6. Dielectric characterization of oxide thin films
7. Setup and verification of a hydrogen etching system for substrate surface preparation

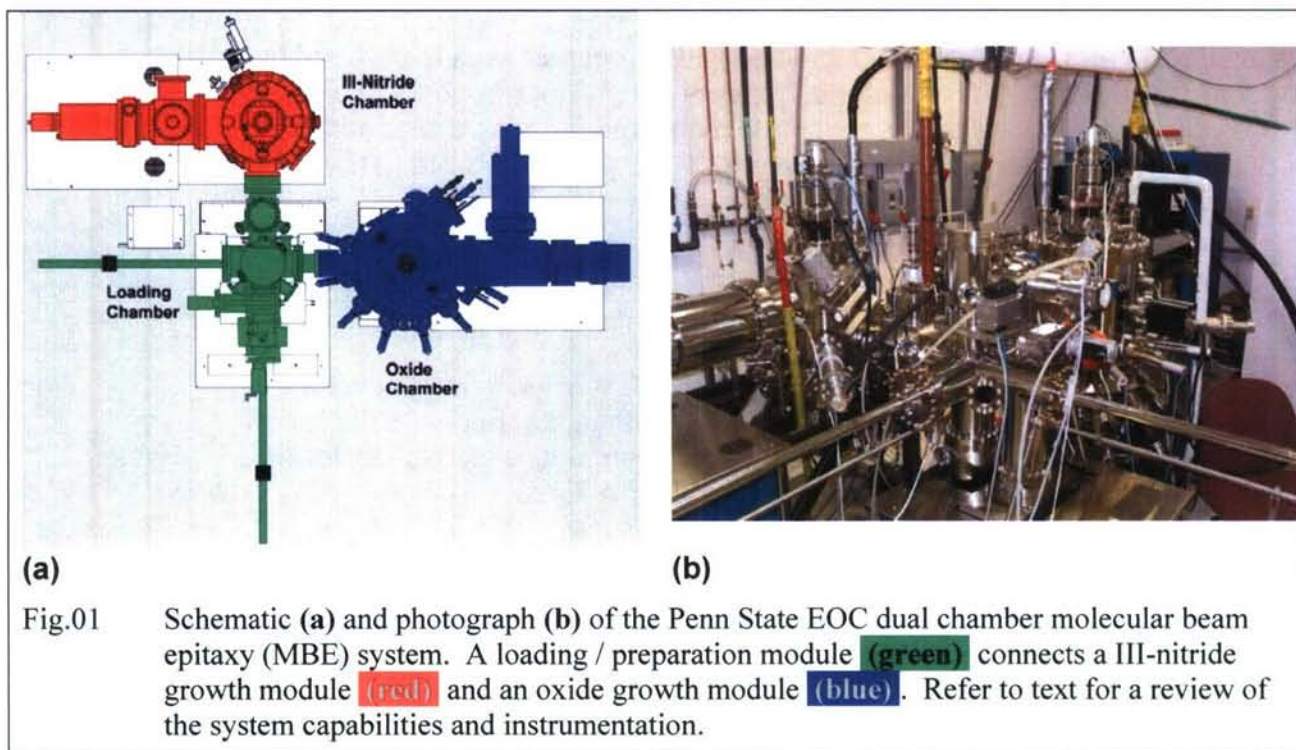
Elements of the abovementioned activities involved close collaboration with Dr. Marek Skowronski, Dr. Paul Salvador and graduate student Patrick Fisher (Carnegie Mellon University, Department of Materials Science and Engineering – CMU DMSE), Dr. Joan Redwing, Dr. Xiaojun Weng and graduate students Dan Perez and Jeremy Acord (Penn State University, Department of Materials Science and Engineering – PSU DMSE), Dr. Mike Lanagan and graduate student Lance Haney (Penn State University, Materials Research Laboratory – PSU MRL), Dr. Jian Xu and graduate student Matthew Snyder (Penn State University, Department of Engineering Science and Mechanics – PSU ESM).

Molecular beam epitaxy (MBE) has been selected to address the challenges mentioned above. Atomic layer deposition by MBE grants precise control of the layer stoichiometry, nucleation and interface chemistry. The ultra-high vacuum ambient used for MBE runs permits enhanced control of potential contaminants and eliminates undesired interaction of reactive species amongst themselves or with ambient species. Being a non-equilibrium process, molecular beam epitaxy enables the growth of “impossible” / incompatible layer systems, i.e. layer systems that would not be stable near the thermal equilibrium.

Molecular Beam Epitaxy System – Equipment, Capabilities and Infrastructure

The Penn State Electro-Optics Center's MBE system was custom-designed by SVT Associates (SVT) to accommodate the sequential deposition of III-nitride and advanced oxide films in dedicated growth modules (Fig. 01) to ultimately accommodate the integration of functional III-nitride and advanced oxide epitaxial layers for RF electronics applications.

The **load lock module** is designed for 3" diameter substrates, is connected to a turbo molecular pump, features a multi-station sample holder elevator. The module is used to facilitate the transfer of substrates and substrate holders into the nitride or oxide growth module under UHV conditions. The sample preparation module is evacuated using an ion pump and permits substrate surface desorption utilizing a 600°C heater to clean substrate surfaces prior to growth.



The **III-nitride MBE growth module** is designed for 3" diameter substrates, is connected to a CTi cryosorption pump and features a pyrolytic graphite heater capable of 1200°C operation. Effusion cells (SVT) provide matrix elements (Ga, Al, In) and dopants (Si, Mg). An SVT RF plasma source is used to provide elemental nitrogen and an SVT thermal cracker cell can be used for hydrogen injection. Reflected high-energy electron diffraction (RHEED) (Staib Instruments / Specs) is used for *in-situ* growth monitoring. A mass-spectrometric residual gas analyzer (MKS) permits *in-situ* gas composition analysis. An UV-vis spectrometer (Ocean Optics) can be employed to monitor the nitrogen plasma emission during the epitaxy runs. The source flux is measured with a retractable ion gauge flux monitor (SVT). A multi-beam optical stress sensor (MOSS) system (kSpace Associates) (Fig. 03), explained in more detail below, is used for *in-situ* tracking of the curvature of substrate and epitaxial layers.

The **oxide MBE growth module** is designed for 3" diameter substrates and is evacuated by a high flux Pfeiffer turbo molecular pump. A pyrolytic boron nitride heater allows to heat the

substrate to 1000°C during the epitaxy runs. Effusion cells (SVT) provide perovskite and rocksalt matrix elements (Ti, Ba, Sr, Mg). An e-gun evaporator (MDC) can be used to transport solid, pre-mixed targets (Ti, TiO₂, BaO, SrO). The oxygen is provided by an integrated ozone source / generator (SVT) at flux rates up to 10⁻⁴. *In-situ* analysis instrumentation includes a RHEED system (Staib Instruments / Specs), a residual gas analyzer (MKS / ExTorr), an ion gauge flux monitor (SVT) and a crystal quartz deposition monitor (MKS).

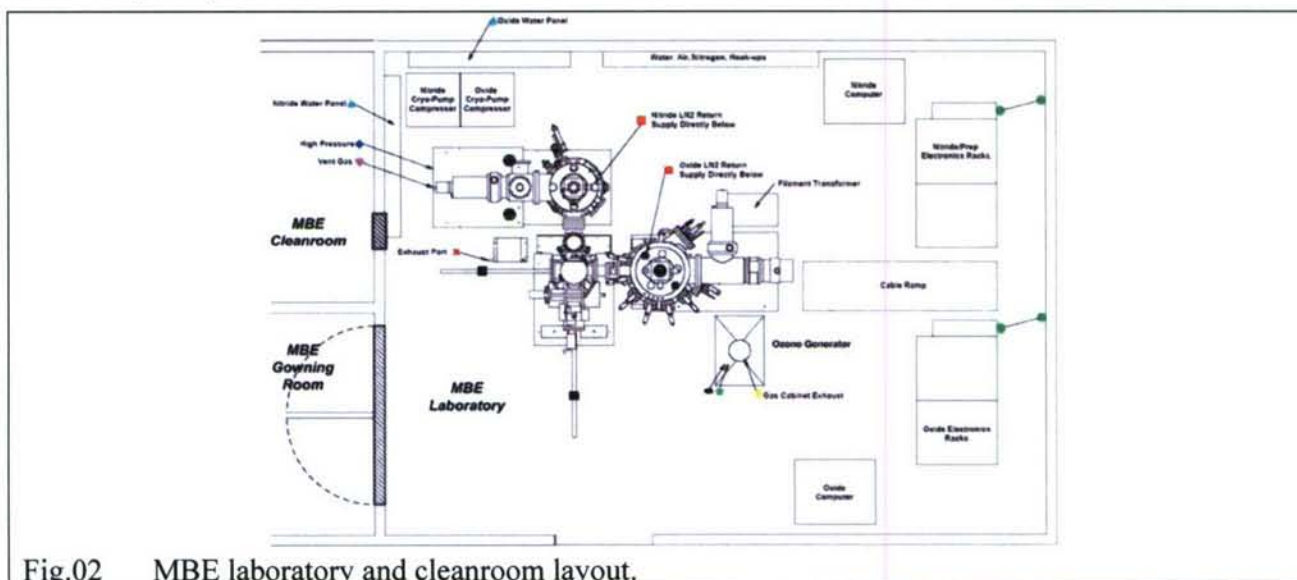


Fig.02 MBE laboratory and cleanroom layout.

A dedicated sample preparation clean room has been established adjacent to the MBE growth laboratory to facilitate substrate cleaning prior to MBE growth experiments (Fig. 02). A bulk liquid nitrogen tank and supply system, a dedicated heat exchanger pump station tying the MBE coolant system into the facilities chiller system, and a 30kVA uninterruptible power supply system have been installed to assure MBE operation.

The III-nitride growth module is equipped with a **multibeam optical stress sensor (MOSS) system** (*kSpace Associates, kSA*) for *in-situ* tracking of the surface curvature of the substrate and/or epitaxial layers (Fig. 03). The growth surface is continuously illuminated near its normal vector by a 1D or 2D matrix of laser dots created by passing a solid state laser beam through an etalon. The dot pattern is monitored under a nearly normal direction over the course of the growth experiment with a CCD area detector. The relative spacing of selected dots and the individual dot intensities are measured as a function of growth duration using kSA's proprietary *Safire* equipment control, image acquisition, data acquisition, and data analysis software (Fig. 03(a)). The information derived from the dot spacing evolution delivers a 1D or 2D surface curvature matrix, which can be transformed into stress-thickness plots using Stoney's equation [8]. For a known layer thickness, the stress-thickness information can be used to calculate cumulative stress information, often referred to as growth stress, which is plotted as a function of growth duration (Fig. 03(b)) or as a function of layer thickness. The intensity of the individual MOSS reflections can be used to deduct the thickness of the grown thin films from the intensity fluctuations based on laser interference in the growing layers. The MOSS system was purchased and installed during the current reporting period and is being used for the evaluation of III-nitride growth experiments. Results from MOSS studies will be discussed in the next reporting period.

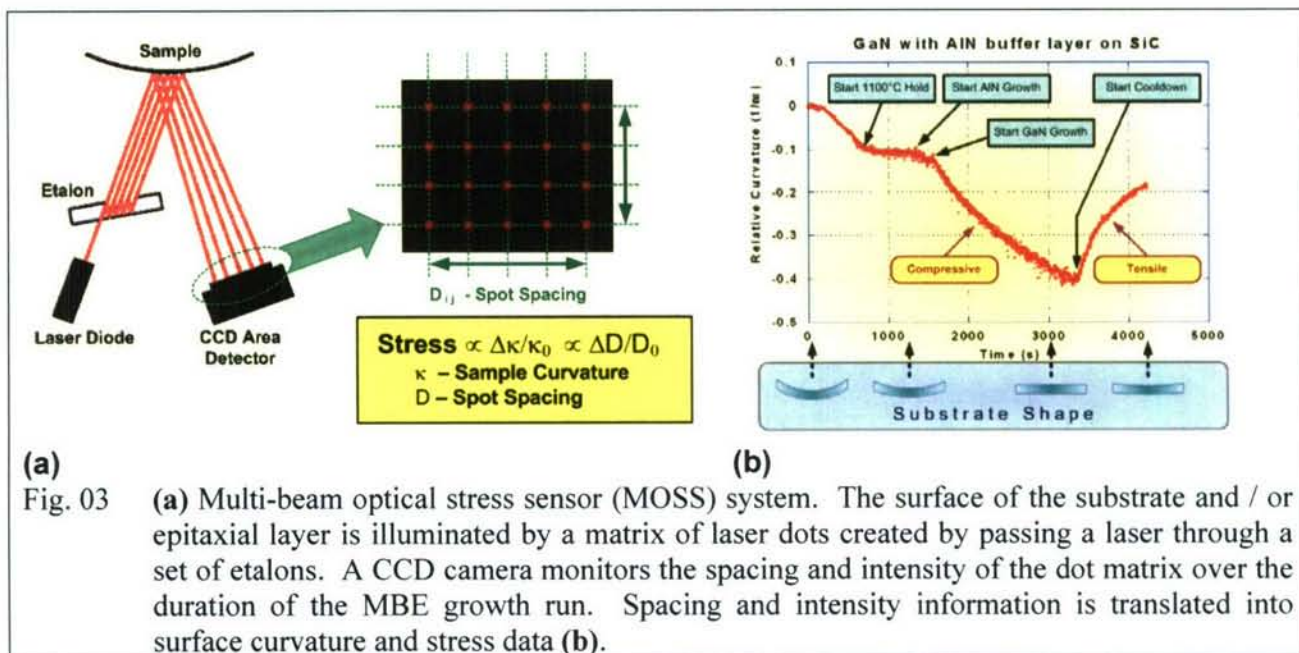
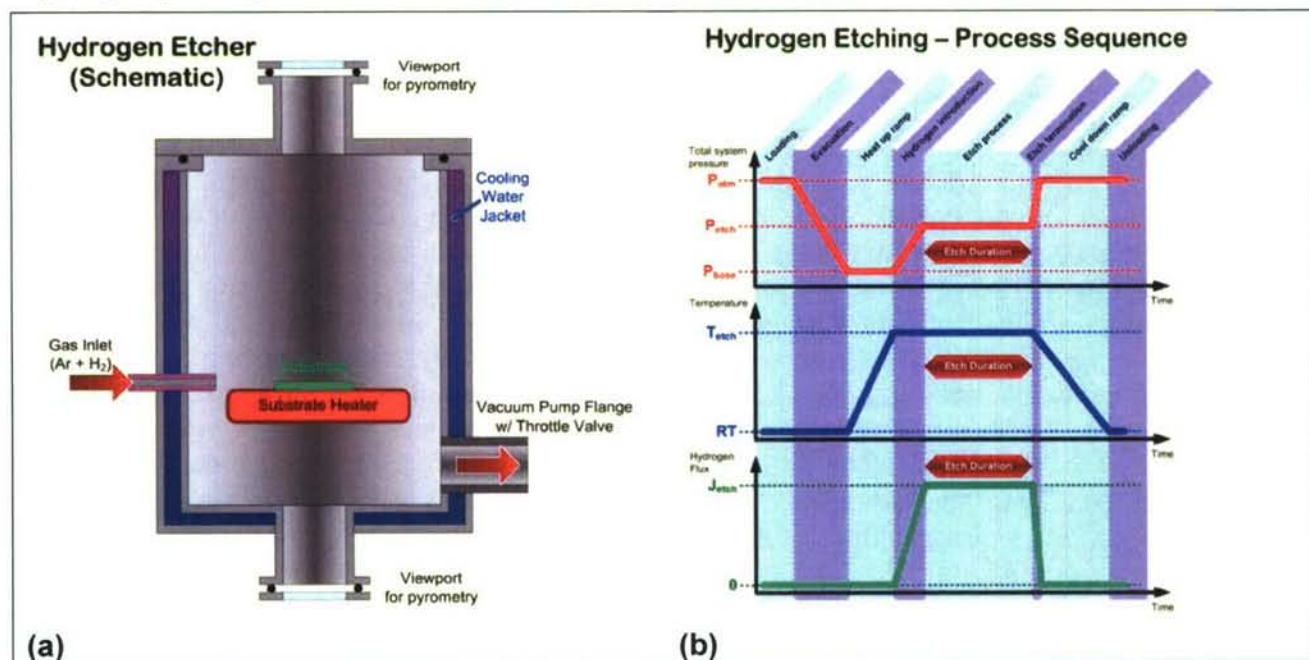


Fig. 03 (a) Multi-beam optical stress sensor (MOSS) system. The surface of the substrate and / or epitaxial layer is illuminated by a matrix of laser dots created by passing a laser through a set of etalons. A CCD camera monitors the spacing and intensity of the dot matrix over the duration of the MBE growth run. Spacing and intensity information is translated into surface curvature and stress data (b).

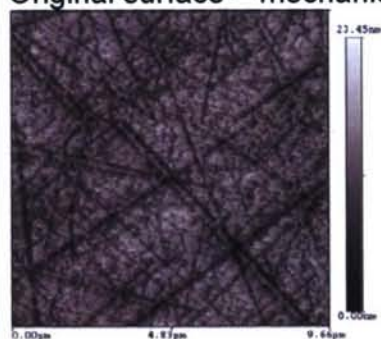
A simple **hydrogen etching system** has been designed and commissioned to allow for the *ex-situ* preparation of clean atomically flat substrate surfaces for MBE epitaxy substrates (Fig. 04). The system consists of a vacuum chamber with a resistive substrate heater, typically a boat-shaped tantalum strip, and a gas handling and vacuum system permitting the introduction of a hydrogen / argon mixture at defined flow rate, total system pressure and hydrogen partial pressure.



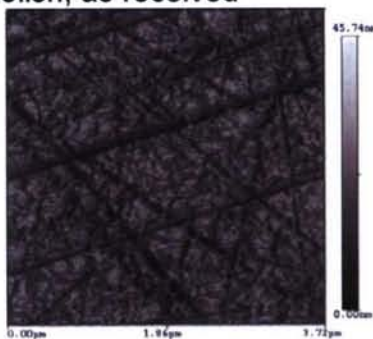


(c) (d)
Fig. 04 Hydrogen etching system (a – schematic, b – typical process sequence, c – vacuum chamber, d – etcher assembly) for the ex-situ preparation of clean, atomically flat substrate surfaces for MBE growth experiments.

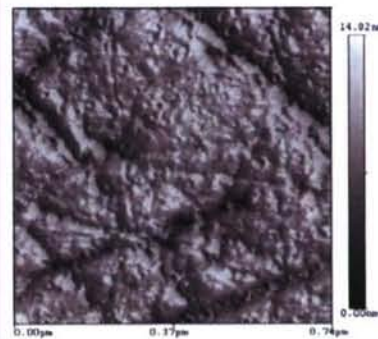
Original surface – mechanical polish, as received



9.66 x 9.66 μm^2

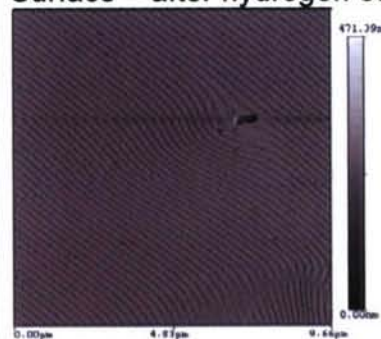


3.72 x 3.72 μm^2

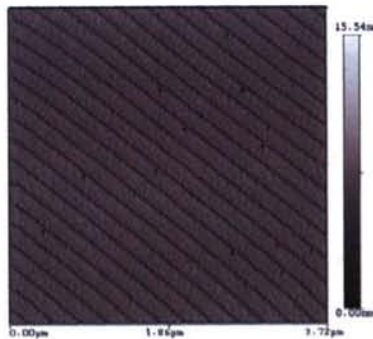


0.74 x 0.74 μm^2

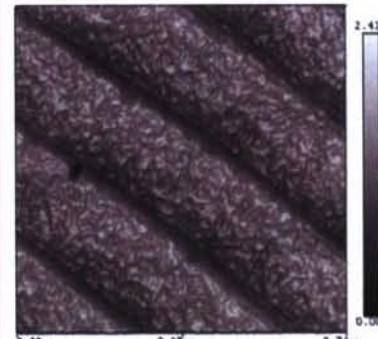
Surface – after hydrogen etch



9.66 x 9.66 μm^2



3.72 x 3.72 μm^2



0.74 x 0.74 μm^2

Fig. 05 Atomic force microscopy images of semi-insulating 6H SiC (0001), nominally on-axis, as-received (top row) and after hydrogen etch at 1600C for 60min at 650 Torr. After hydrogen etch, residual scratches induced by mechanical abrasive polishing are removed. The hydrogen-etched surface exhibits unit-cell height steps and terraces.

Fig. 05 shows an example of a semi-insulating 6H SiC (0001) substrate surface imaged by atomic force microscopy (AFM). The top row shows AFM surface scans at different magnification prior to hydrogen etching, the bottom row, respectively, shows the same wafer surface after hydrogen etching. The residual scratches induced by mechanical abrasive polishing are removed, and the surface exhibits atomically flat terraces. Based on this data, each SiC substrate used for MBE growth experiments (unless noted otherwise) has been subjected to a hydrogen etching to create a repeatably clean and smooth surface finish prior to growth.

The growth of III-nitride epitaxial layers for optoelectronics and RF electronics applications is a well-established process, which has been the subject of over a decade of research and development efforts in the wide bandgap (WBG) materials community, and currently yields commercial grade epitaxial layers. The motivation to establish in-house III-nitride growth capabilities was the necessity to produce device quality epitaxial layers with a well-documented process history. These layers will be used for the future efforts on the integration of WBG materials and device technology with the growth process for tunable oxides.

In order to reach the goal of integrating tunable oxides directly with III-nitride-based RF transistors the efforts have been segregated into three areas:

- A** Development of III-nitride epitaxy for $\text{Al}_x\text{Ga}_{1-x}\text{N}$ high electron mobility transistors (HEMTs)
- B** Development of BST epitaxy for RF tunable capacitors
- C** Integration of oxide and III-nitride epitaxy

Efforts **(A)** and **(B)** are currently ongoing as parallel tasks, as the MBE system layout permits simultaneous, independent III-nitride and oxide growth experiments. Current activities under effort **(C)** encompass the development of MgO epitaxy to be used as interface layers between tunable oxides and the underlying WBG substrate or template. The main tasks on the oxide / III-nitride integration (effort **(C)**) will commence upon demonstration of HEMT quality III-nitride layer growth and tunable oxide layer growth suitable for RF varactors.

III-nitride epitaxy for $\text{Al}_x\text{Ga}_{1-x}\text{N}$ high electron mobility transistors (HEMTs)

The strategy for III-nitride growth experiments continues to follow the straightforward route towards a demonstration of $\text{Al}_x\text{Ga}_{1-x}\text{N}$ high electron mobility transistors (HEMTs), a device architecture to be combined with tunable oxide layers for the evaluation of properties and issues in the direct integration WBG / oxide RF devices on the same substrate.

Basic $\text{Al}_x\text{Ga}_{1-x}\text{N}$ HEMTs consist of a semi-insulating substrate (typically on-axis SI SiC), a ~50nm thick AlN buffer layer, a ~1 to 3 μm thick GaN layer, and a ~30nm thick $\text{Al}_x\text{Ga}_{1-x}\text{N}$ layer with approximately 27% aluminum content. The initial device designs will not utilize surface passivation layers. Dr. Joseph Flemish at PSU DMSE is currently investigating AlGaIn HEMT passivation strategies that will be applied to EOC's HEMT wafers in the future.

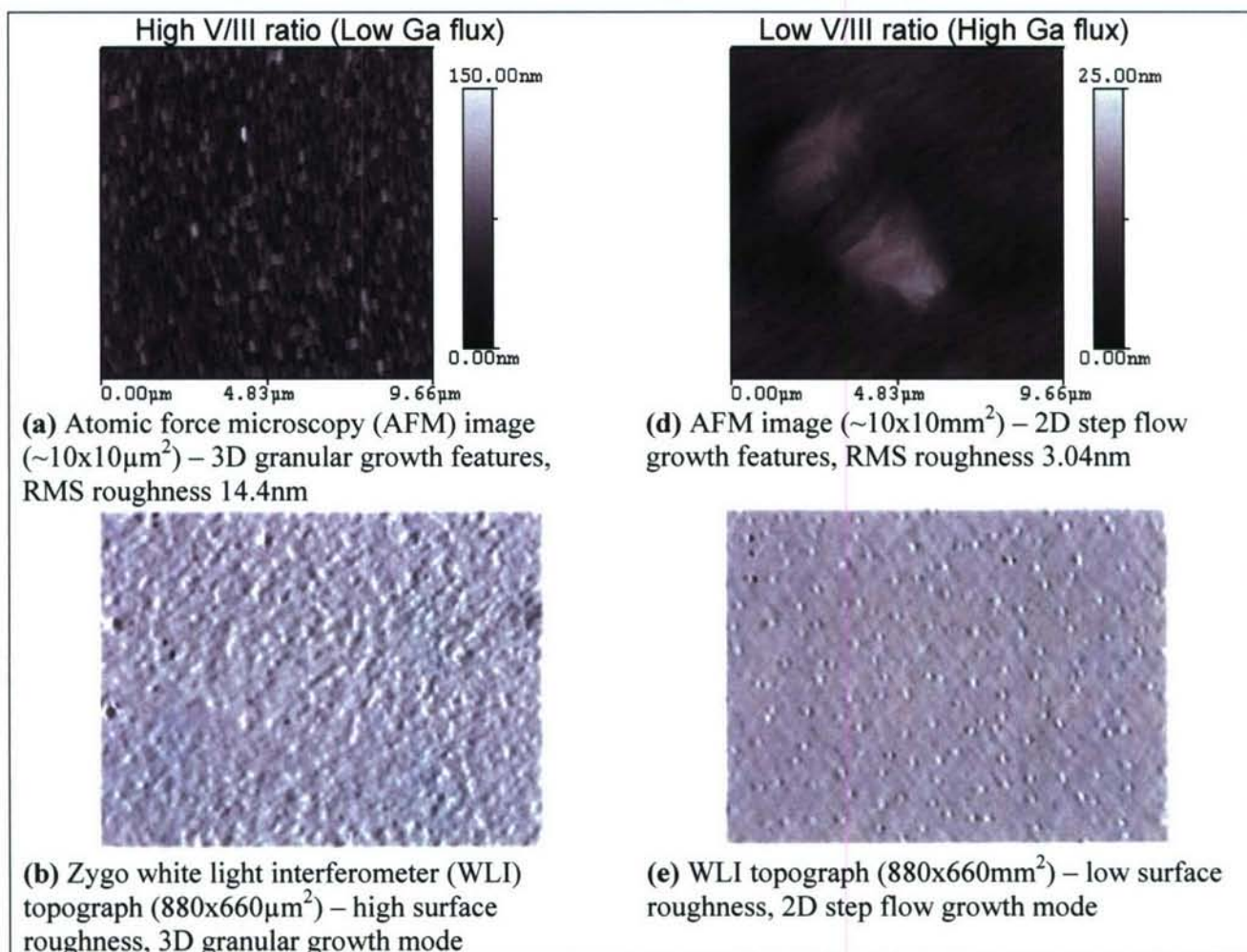
The III-nitride epitaxial development plan encompasses the following stages and milestones:

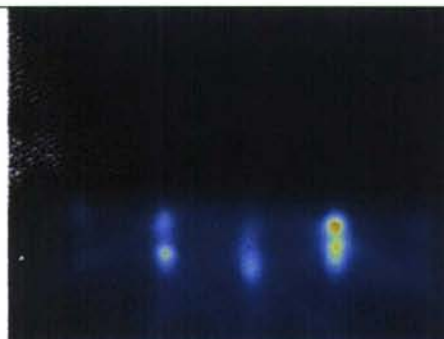
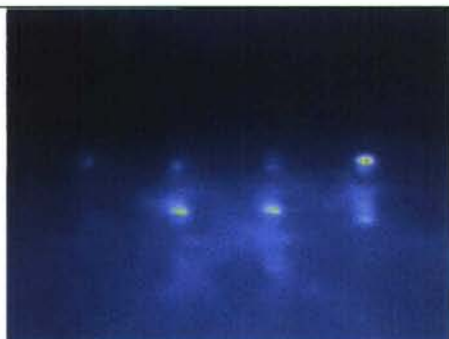
- A1** Growth of AlN epitaxial buffer layers on SI SiC substrates (AlN/SiC structure)
- A2** Growth of not-intentionally doped GaN epitaxial layers on AlN/SiC (GaN/AlN/SiC structure)
- A3** Growth of $\text{Al}_x\text{Ga}_{1-x}\text{N}$ epitaxial layers on GaN/AlN/SiC (HEMT structure)

Initial AlN and GaN growth experiments under effort **A1** were conducted on readily available Si and GaAs substrates instead of expensive SiC substrates to establish source flux

calibrations. The AlN, GaN and AlGaIn growth processes are being transitioned to hydrogen-etched SI 6H (0001) SiC and SI 4H (0001) SiC substrates in the follow-on period. The GaN / AlGaIn interface quality, the composition and Al content of the AlGaIn layer, as well as growth-induced stress in the SiC / AlN / GaN / AlGaIn epitaxial layer stack greatly impact the performance and reliability of HEMT devices structured from such layers. *In-situ* RHEED is used to monitor the properties of the GaN / AlGaIn interface. *In-situ* MOSS measurements record the surface curvature of the substrate / epitaxial layer system over the course of an MBE run, which can be translated into cumulative relative stress data. *Ex-situ* HRXRD is used to quantify both the AlGaIn layer composition and room temperature stress.

Due to difficulties filling the graduate student positions for III-nitride and oxide growth and characterization some of the tasks were delayed during the initial 6 to 9 months of the reporting period. Graduate student D.Perez (PSU DMSE) started work on the III-nitride development task in Jan-2006 and graduate students P.Fisher and M.Snyder started work on the oxide development effort in Dec-2005 and Aug-2006, respectively.





(c) “Spotty” (11-20) RHEED pattern indicates high surface roughness of growing GaN layer, 3D granular growth mode

(f) “Streaky” (11-20) RHEED pattern indicates low growth surface roughness, 2D step flow growth mode

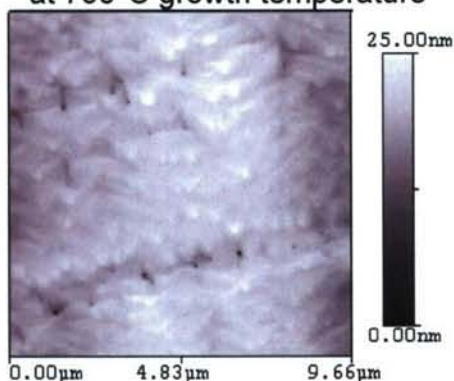
Fig. 06 Comparison of AFM scans (a/d), WLI topographs (b/e) and *in-situ* RHEED patterns (c/f) of GaN layers grown at high (a/b/c) and low (d/e/f) V/III ratio, respectively. Refer to notes next to respective part of this figure for details.

Initial gallium nitride (GaN) runs were conducted on silicon substrates. A series of experiments investigated the impact of the V/III ratio on the crystal quality and morphology of the growing layer. Figure 06 shows examples of GaN layers grown at high (Fig. 06 a, b, c) and low (Fig. 06 d, e, f) V/III ratio, facilitated by low and high gallium flux, respectively.

Fig. 06 a and d show atomic force microscopy (AFM) scans of $9.66 \times 9.66 \mu\text{m}^2$ areas representative of the GaN epitaxial layers' morphology. The layer grown under high V/III ratio exhibits a granular morphology with a rms roughness of 14.4 nm (Fig. 06 a), whereas the layer grown under low V/III ratio has a rms roughness of 3.04 nm and exhibits step flow growth (Fig. 06 d). Zygo NewView white light interferometry conducted on these layers delivers topographs of $880 \times 660 \mu\text{m}^2$ areas of these layers confirming the rough morphology of the sample grown under high V/III ratio (Fig. 06 b) and step flow morphology of the sample grown under low V/III ratio (Fig. 06 e). These observations agree with the (11-20) RHEED patterns collected on the samples grown under high (Fig. 06 c) and low (Fig. 06 f) V/III ratio, showing “spotty” and “streaky” patterns, respectively, which indicate high surface roughness and 3D island / granular growth mode for high V/III ratio and low surface roughness and 2D step flow growth mode for low V/III ratio.

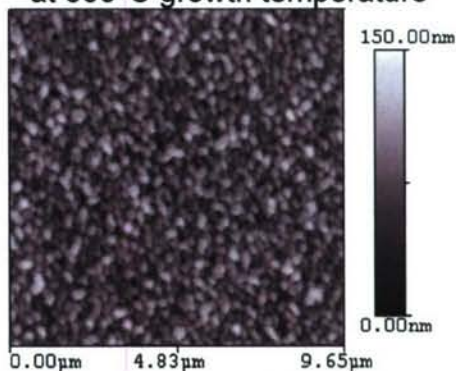
Another critical growth parameter is the substrate temperature during the deposition of the GaN epitaxial layer since it determines the mobility of the adsorbed matrix species, the growth mode (between granular growth, step flow growth and thermal re-desorption of the epitaxial layer) and the crystal quality. Fig. 07 shows results from GaN growth runs on silicon substrates conducted at growth temperatures of 700°C and 800°C, bracketing the critical point of thermal re-desorption of the deposited layer. The layer morphology changes back from step flow growth of a continuous, smooth GaN layer as indicated by AFM (Fig. 07 a / d) and RHEED (Fig. 07 b / e). In order to determine the range of growth parameters permitting step flow growth of continuous, stoichiometric III-nitride epitaxial layers, the parameter space of substrate temperature and V/III ratio was mapped for silicon (Si) substrates in the initial set of experiments. Current experiments repeat these studies for growth of AlN and GaN epitaxial layers on semi-insulating silicon carbide (Si-SiC) substrates.

High growth rate $0.81\mu\text{m/h}$
at 700°C growth temperature



(a) Atomic force microscopy (AFM) image ($\sim 10 \times 10\mu\text{m}^2$) – 2D step flow growth features, RMS roughness 2.69nm

Low growth rate $0.45\mu\text{m/h}$
at 800°C growth temperature



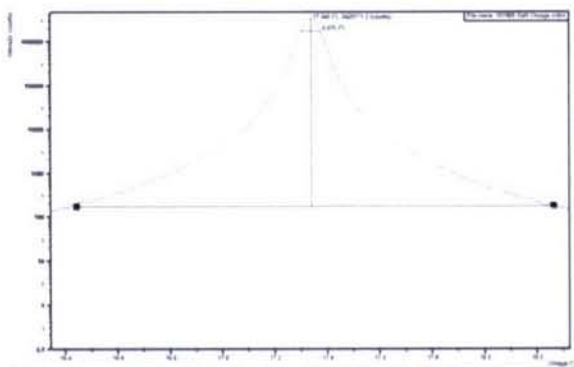
(d) AFM image ($\sim 10 \times 10\mu\text{m}^2$) – 3D granular flow growth features, RMS roughness 19.9nm



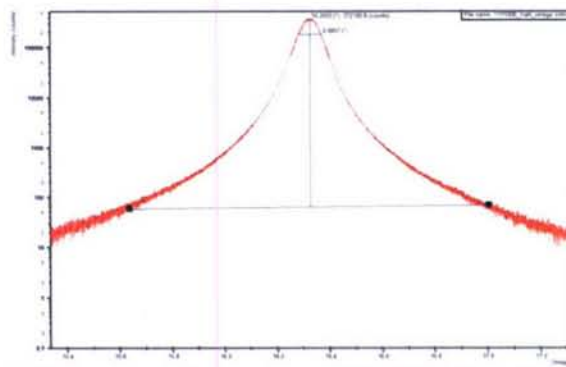
(b) “Streaky” (11-20) RHEED indicates low growth surface roughness, 2D step flow growth mode



(e) “Spotty” (11-20) RHEED pattern indicates high surface roughness of growing GaN layer, 3D granular growth mode



(c) X-ray rocking curve of GaN (002) peak exhibiting a full width of half maximum (FWHM) of 270 arcsec.



(f) X-ray rocking curve of GaN (002) peak exhibiting a FWHM of 315 arcsec.

Fig. 07 Comparison of AFM scans (a/d), *in-situ* RHEED patterns (b/e) and x-ray rocking curves (c/f) of GaN layers grown at low growth temperature (700°C) / high growth rate ($0.81\mu\text{m/h}$) (a/b/c) and high growth temperature (800°C) / low growth rate ($0.45\mu\text{m/h}$) (d/e/f), respectively. Refer to notes next to respective part of this figure for details.

A substrate temperature increase from 700°C to 800°C resulted in a ~2x reduction in growth rate, indicating the onset of thermal decomposition of the deposited GaN layer which is also visible in the surface morphology change of the respective epitaxial layers.

The III-nitride epitaxy work has since been transitioned to growth of AlN and GaN on semi-insulating silicon carbide (SI SiC) substrates. Results from these growth studies will be discussed in the next reporting period.

Tunable oxide epitaxy for RF tunable capacitors

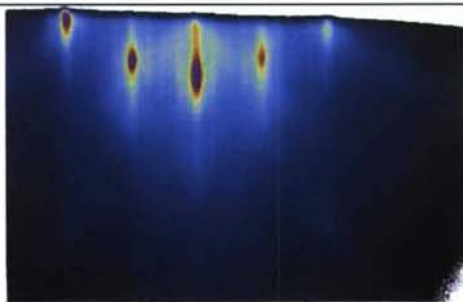
The development of ferroelectric tunable oxide layers commenced during the reporting period, in parallel to the III-nitride growth process development, based on the following experimental plan:

- | | |
|-----------|---|
| B1 | Growth of TiO ₂ epitaxial layers on oxide substrates |
| B2 | Growth of SrTiO ₃ epitaxial layers on oxide substrates |
| B3 | Growth of BaTiO ₃ epitaxial layers on oxide substrates |
| B4 | Growth of Ba _x Sr _{1-x} TiO ₃ epitaxial layers on oxide substrates |
| B5 | Growth of MgO buffer layers |

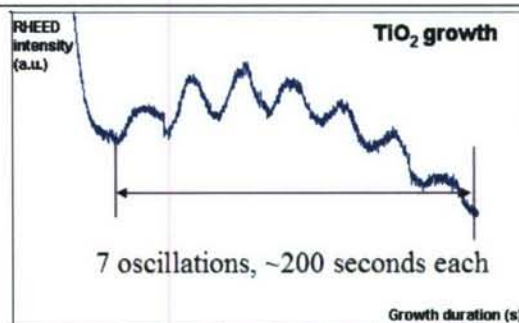
Titanium dioxide (TiO₂) deposition studies under effort **B1** were used to calibrate the Ti and O fluxes and develop a nucleation process on oxide substrates. By addition of strontium and barium, in two separate studies, growth processes for STO (strontium titanate, SrTiO₃) under effort **B2** and BTO (barium titanate, BaTiO₃) under effort **B3** were developed for oxide substrates. Initial demonstrations of BST (barium strontium titanate, Ba_xSr_{1-x}TiO₃) growth under effort **B4** were completed during the reporting period. These BST layers will undergo dielectric characterization and device fabrication in the upcoming reporting period.

MBE Growth of TiO₂

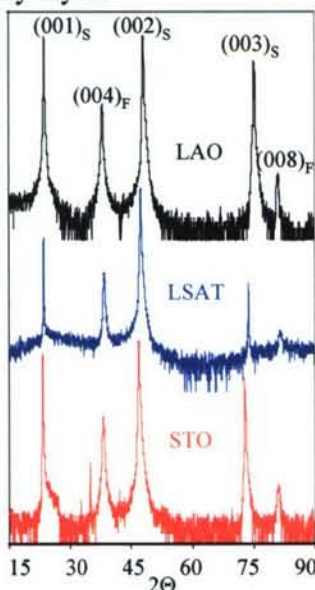
The initial oxide growth experiments were designed to develop a stable deposition process for TiO₂, the core matrix of more complex perovskite oxides such as STO (SrTiO₃), BTO (BaTiO₃) and BST (Ba_xSr_{1-x}TiO₃). The MBE system uses an ozone-enriched oxygen injection source, i.e. operates under oxygen-rich conditions. Thus the determination and calibration of the titanium flux was critical to map out growth conditions that yield stoichiometric TiO₂ thin films. The initial TiO₂ growth experiments were conducted on oxide substrates such as STO (strontium titanate, SrTiO₃), LSAT ((La_{0.29},Sr_{0.71})(Al_{0.65},Ta_{0.35})O₃) and LAO (lanthanum aluminate, LaAlO₃) to investigate the impact of the substrate lattice mismatch on the nucleation, growth morphology, crystal modification (rutile vs. anatase), crystal quality and stoichiometry of the epitaxial TiO₂ layers deposited under a variety of growth conditions. The Ti/O ratio was varied by changing the Ti effusion cell temperature and the ozone / oxygen flow. Fig. 08 shows representative results of TiO₂ growth experiments.



(a) In-situ RHEED pattern of TiO_2 grown on LAO substrate indicating epitaxial growth mode of high quality layer.



(b) RHEED intensity oscillations of (002) TiO_2 peak over growth duration. Seven oscillations, at 200 s each, were observed. $T_{\text{Ti}} = 1550^\circ\text{C}$



(c) XRD spectra of TiO_2 grown on STO (red curve), LSAT (blue curve) and LAO (black curve).



(d) High resolution cross-sectional transmission electron micrograph (HRXTEM) of anatase TiO_2 deposited on (100) LaAlO_3 .

Fig. 08 MBE-grown TiO_2 epitaxial films on STO, LSAT and LAO substrates, characterized by (a) in-situ RHEED pattern, (b) in-situ RHEED peak intensity oscillations, (c) x-ray diffraction and (d) HRXTEM. Refer to notes next to respective part of this figure for details.

The crystal structure of the deposited TiO_2 modification (anatase versus rutile) depends on the substrate (as shown in Fig. 09) and the growth conditions.

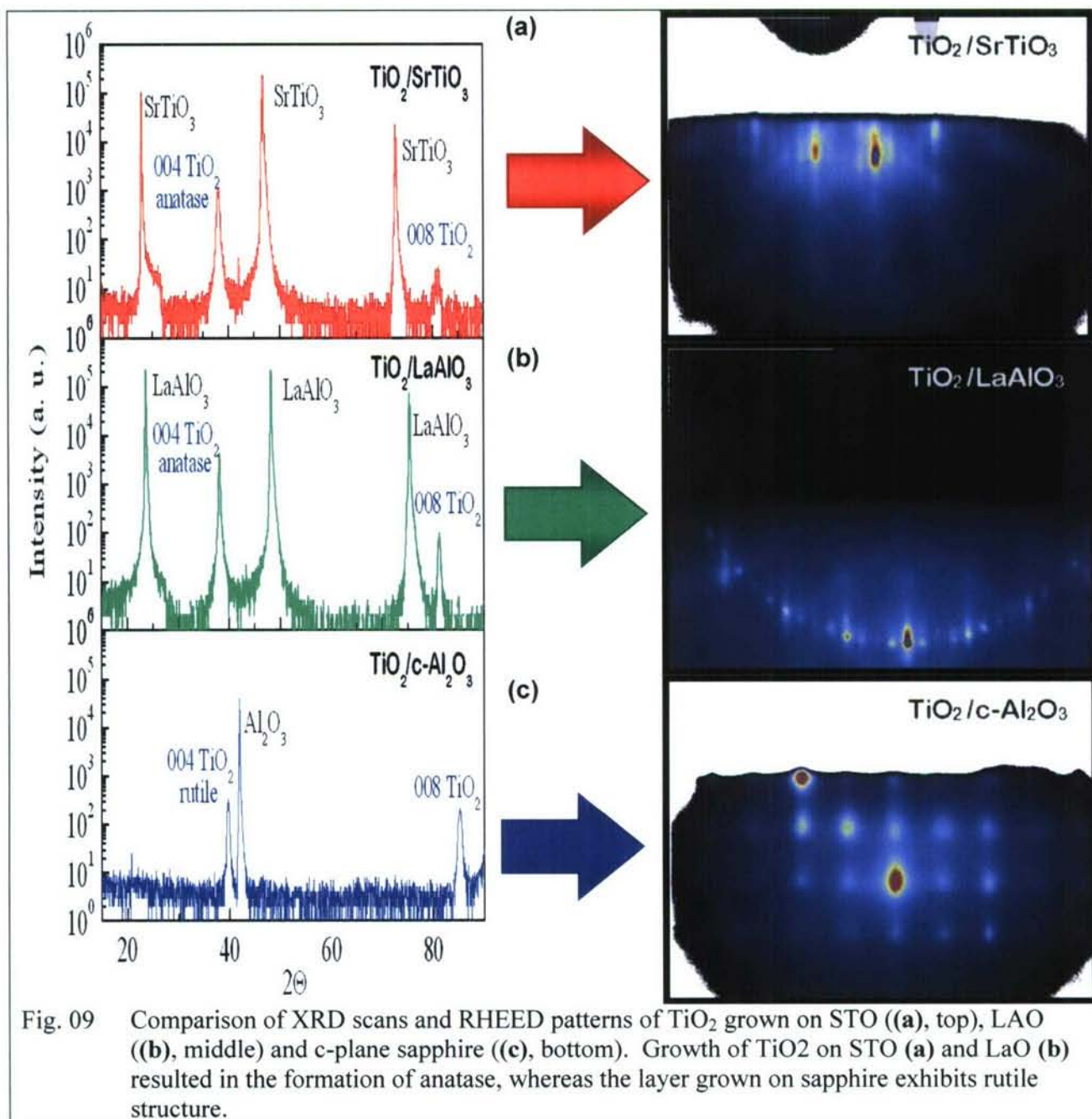


Fig. 09 Comparison of XRD scans and RHEED patterns of TiO_2 grown on STO ((a), top), LAO ((b), middle) and c-plane sapphire ((c), bottom). Growth of TiO_2 on STO (a) and LaO (b) resulted in the formation of anatase, whereas the layer grown on sapphire exhibits rutile structure.

The TiO_2 layer deposited on LAO is anatase and exhibits high crystal quality and a sharp, low defect interface as depicted in the XTEM micrographs in Fig. 10.

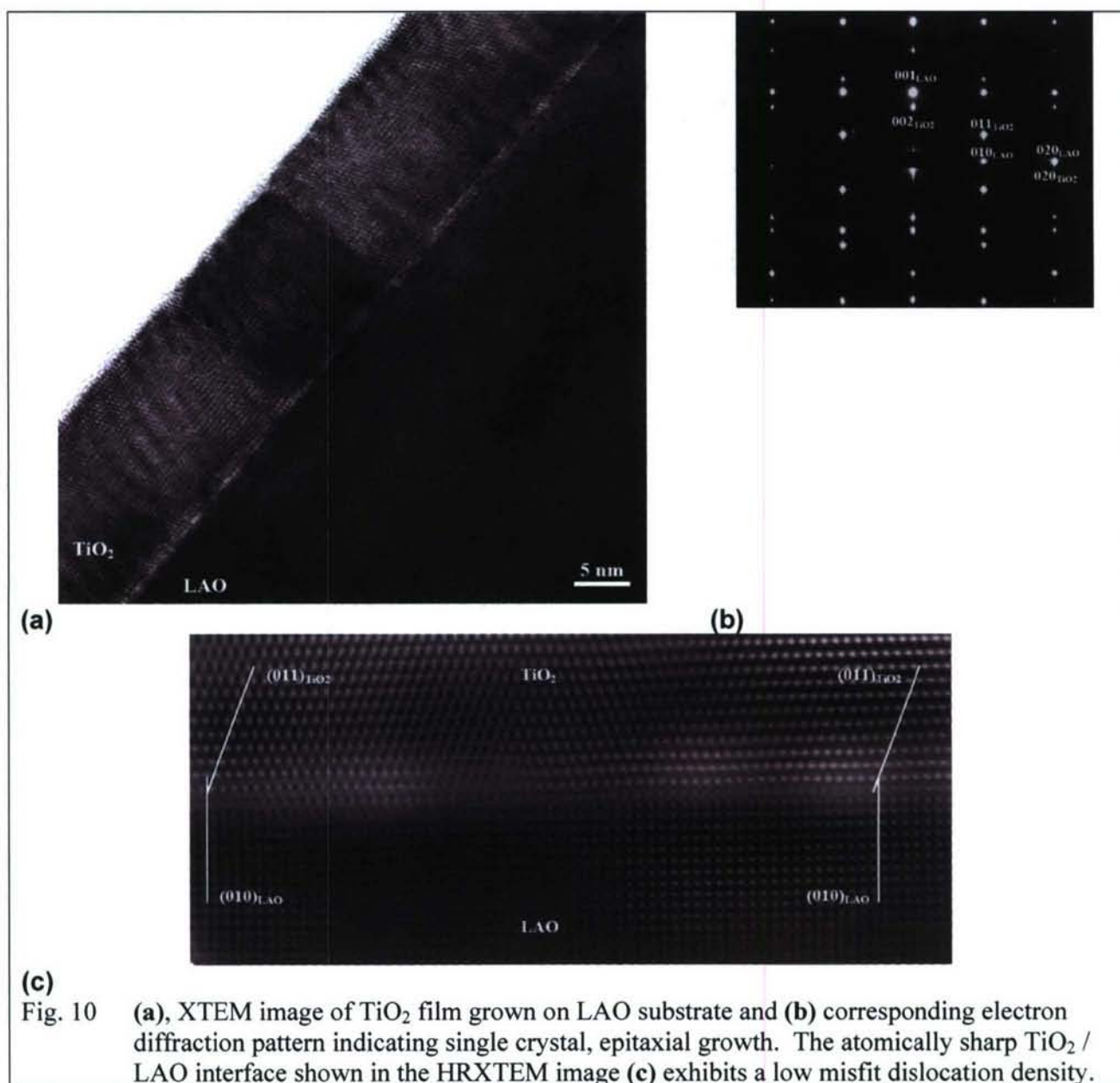
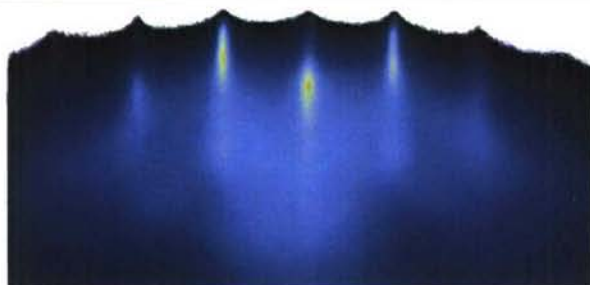


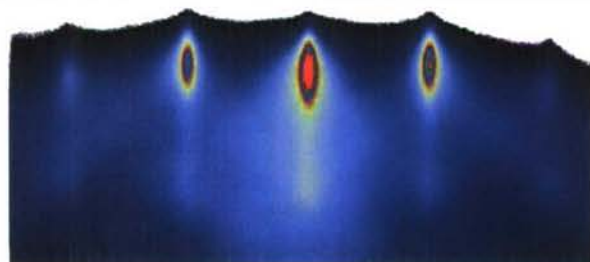
Fig. 10 (a), XTEM image of TiO₂ film grown on LAO substrate and (b) corresponding electron diffraction pattern indicating single crystal, epitaxial growth. The atomically sharp TiO₂ / LAO interface shown in the HRXTEM image (c) exhibits a low misfit dislocation density.

MBE Growth of SrTiO₃

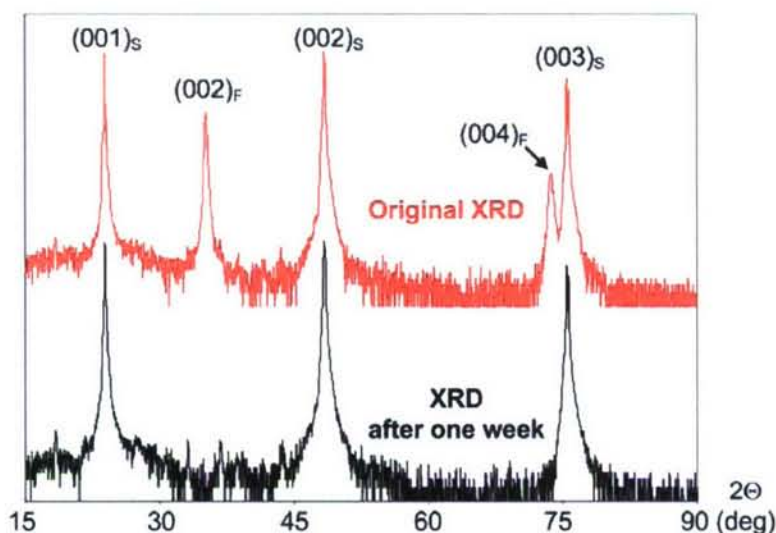
The next step towards a BST growth process was the exploration of suitable growth conditions for STO. The strontium flux calibration was conducted in growth experiments depositing SrO. Fig. 11 shows the RHEED patterns in the (110) azimuth (a) and (100) azimuth (b) as well as XRD spectra (c) of as-deposited SrO (red curve) and the same film after storage for one week under dry atmosphere (black curve), indicating a degradation of the film.



(a) RHEED pattern in (110) azimuth of SrO epitaxial layer.



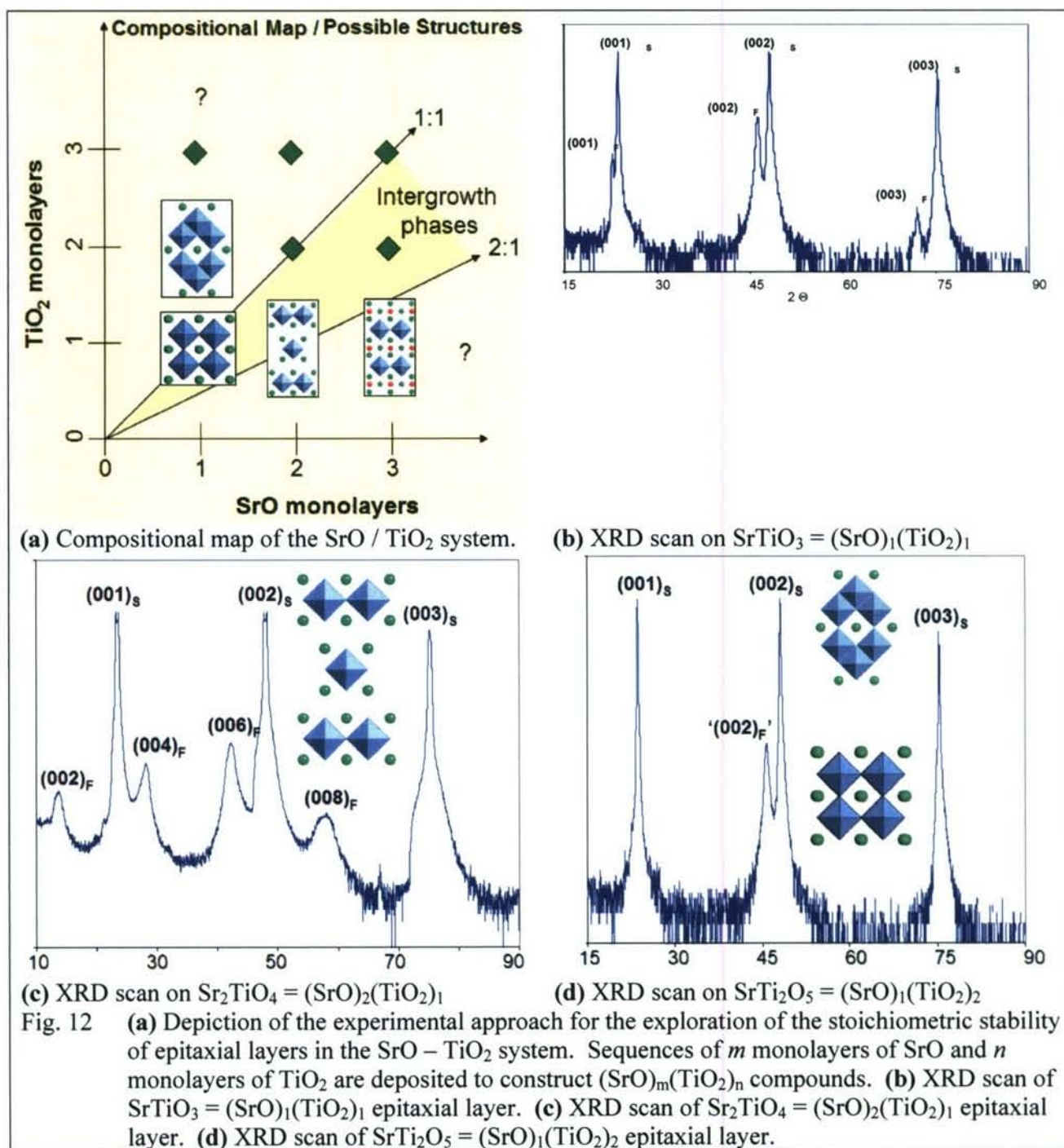
(b) RHEED pattern in (100) azimuth of SrO epitaxial layer.



(c) XRD scan of as-deposited SrO film (red curve) and same film after one week storage in dry atmosphere (black curve) indicating a degradation of the film.

Fig. 11 MBE-grown SrO epitaxial films characterized by (a) RHEED pattern in (110) azimuth, (b) RHEED pattern in (100) azimuth, and (c) XRD scan on as-deposited film (red curve) and the same film after one week storage in dry atmosphere (black curve).

The layer properties of the $(\text{SrO})_m(\text{TiO}_2)_n$ system was explored for a variety of growth conditions based on the native instability of SrO thin films. For that purpose, sets of m SrO and n TiO_2 monolayers were sequentially deposited by atomic layer mode molecular beam epitaxy. Growth behavior, layer properties and layer stoichiometry were characterized as a function of the Sr / Ti ratio determined by the numbers m of SrO monolayers and n of TiO_2 monolayers that were sequentially deposited. Fig.12 a depicts the matrix of m and n values investigated (e.g. $m, n = 0, 1, 2, 3, \dots$). In addition to the depicted integer increments of m and n , the Sr and Ti concentrations during the layer growth were modified in small increments δm and δn ($\delta m, \delta n \ll 1$) around integer values of m and n (e.g. $m + \delta m, n + \delta n = 0.90, 0.95, 1.00, 1.05, 1.10, \dots$).



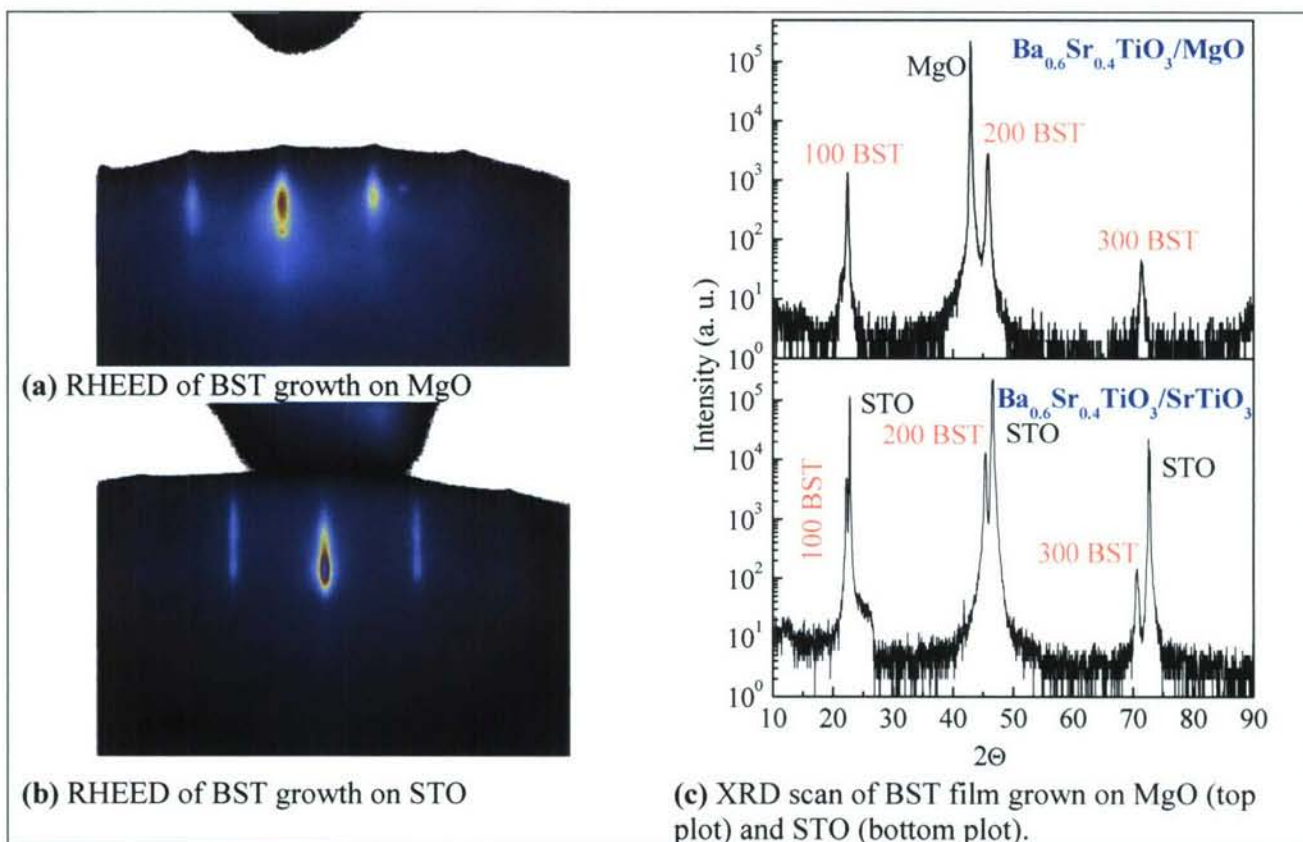
Stable SrTiO₃ thin films have been deposited for (*m* = *n*) values up to 33. The *m* ≠ *n* combinations produce the known stable Ruddlesden-Popper phases. The *m*+δ*m* / *n*+δ*n* study is still in progress; its findings will be discussed in the next reporting period. Preliminary results seem to indicate that all runs with a (*m* = *n*) composition relax into stoichiometric, continuous SrTiO₃ films.

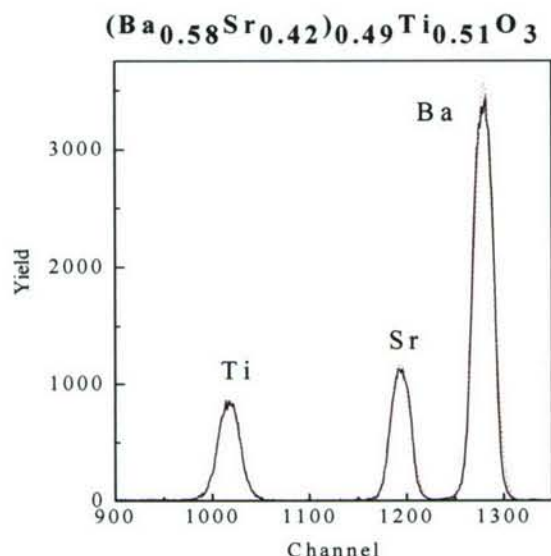
MBE Growth of BaTiO_3

An equivalent study will be conducted for the $(\text{BaO})_p(\text{TiO}_2)_q$ system during the upcoming reporting period.

MBE Growth of $\text{Ba}_x\text{Sr}_{1-x}\text{TiO}_3$

Initial parametric spot checks of BST growth have been completed targeting a $\text{Ba}_{0.6}\text{Sr}_{0.4}\text{TiO}_3$ composition. Fig. 13 shows the RHEED patterns (a, b), XRD scans (c) on BST films grown on MgO (a, c (top plot)) and STO (b, c (bottom plot)) as well as a Rutherford backscattering (RBS) scan (d) of the sample that best matched the targeted stoichiometry.





(d) Rutherford backscattering (RBS) scan of BST epitaxial layer grown on MgO substrate. RBS analysis yields the relative atomic concentrations of Ba, Sr and Ti in the grown BST thin films. The RBS scan on the left shows the best-to-date BST film with a composition of $(\text{Ba}_{0.58}\text{Sr}_{0.42})_{0.49}\text{Ti}_{0.51}\text{O}_3$ or Ba : Sr : Ti = 0.28 : 0.21 : 0.51. The BST film composition targeted in these growth experiments was $\text{Ba}_{0.6}\text{Sr}_{0.4}\text{TiO}_3$.

Note: The resolution of the RBS analysis is quoted as 1% atom concentration.

Fig. 13 RHEED on BST epitaxial layer grown on (a) MgO substrate and (b) STO substrate, XRD scans on BST on MgO ((c), top plot) and StO ((c), bottom plot) and (d) Rutherford backscattering (RBS) scan on BST film with $(\text{Ba}_{0.58}\text{Sr}_{0.42})_{0.49}\text{Ti}_{0.51}\text{O}_3$ composition.

Current efforts focus on the stabilization and repeatability of BST growth and improvements to the stoichiometry control of BST layers. The Ba/Sr ratio in the BST thin films determines their ferroelectric properties which critically impact the behavior of tunable capacitors fabricated from these films.

The oxide community is currently discussing the most suitable metrology method to determine the stoichiometry of such epitaxial oxide thin films, ideally using an *in-situ* characterization technique. RHEED-based EDX, also referred to as "RHEED-TRAXS" [9] has yielded initial encouraging results in the attempt to *in-situ* quantify the stoichiometry of advanced oxide thin films. The option of adding a RHEED-based EXD unit to the MBE's oxide growth module over the course of the next reporting is being evaluated and discussed with the program sponsor.

MgO epitaxy for the integration of tunable oxides on WBG substrates

During the reporting period, graduate Matthew Snyder began the development of epitaxial MgO buffer layers on SiC substrates and III-nitride epitaxial layers, which will serve as an interface for the integration of tunable oxide layers on SiC and / or III-nitrides.

MgO epitaxial layers were deposited on perovskite substrates such as STO, LSAT and LAO, investigating growth mode, surface morphology and crystal quality. Fig. 14 shows a comparison of RHEED patterns of STO (left), LSAT (middle) and LAO (right) substrates prior to (top) MgO epitaxial layer growth, and the same substrates after the deposition of a MgO layer (bottom). The crystal quality determined by RHEED decays as the layer / substrate lattice mismatch increases from STO (7.4%) to LSAT (8.4%) to LAO (10.1%).

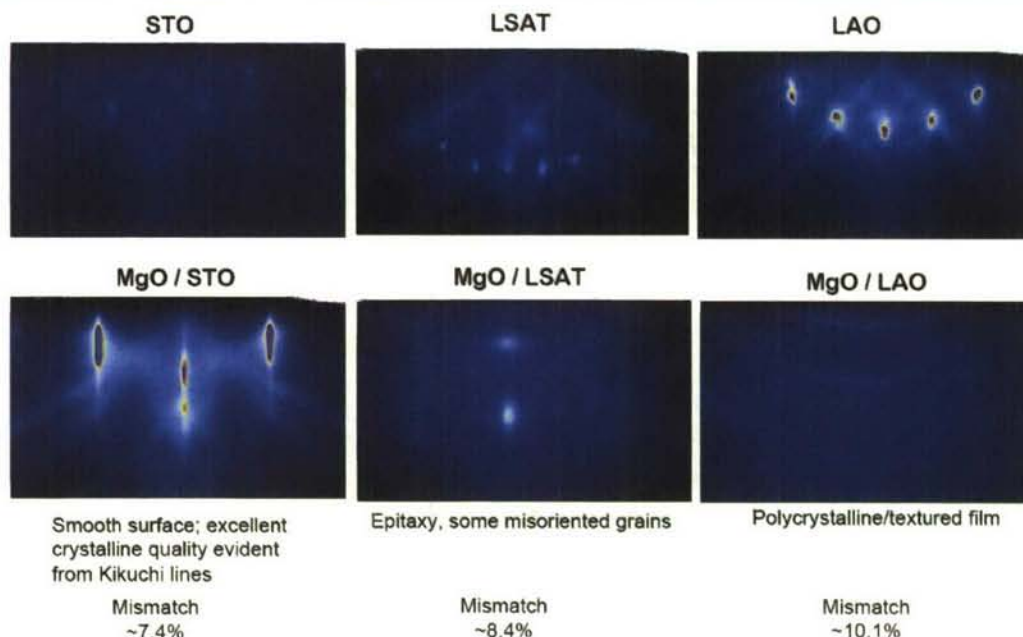


Fig. 14 RHEED patterns of STO (left), LSAT (middle) and LAO (right) substrates prior to (top) MgO epitaxial layer growth, and the same substrates after the deposition of a MgO layer (bottom). RHEED scans indicate a decay in crystal quality as the layer / substrate lattice mismatch increases from STO (7.4%) to LSAT (8.4%) to LAO (10.1%).

To determine the *ex-situ* crystal quality, XRD Θ -2 Θ scans and ω rocking curve scans were performed on these films (Fig. 15). The rocking curve FWHM of the MgO peak increases from 0.36° for STO (top plots) to 0.49° for LSAT (middle plots) to 1.32° for LAO (bottom plots), in accordance with the increasing lattice mismatch.

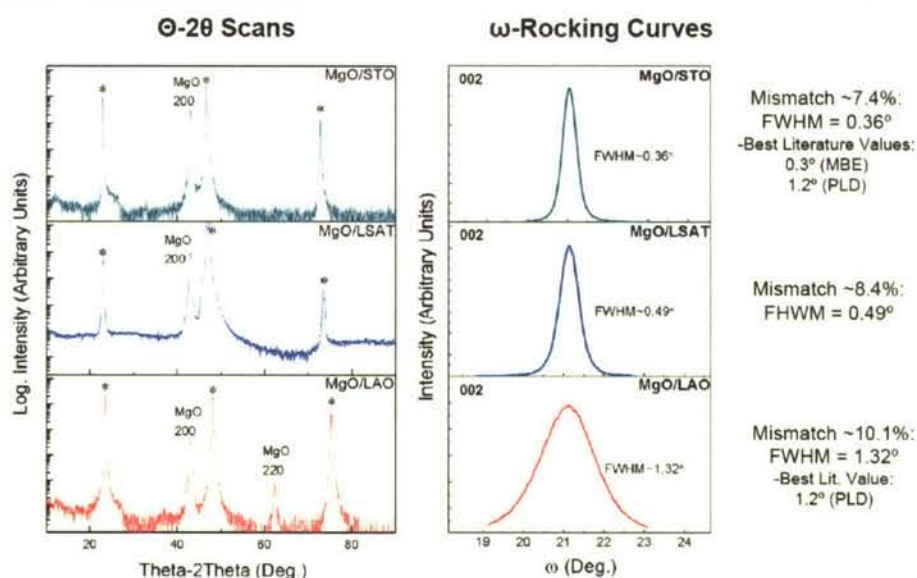


Fig. 15 XRD Θ -2 Θ scans and ω rocking curve scans collected on the films shown in Fig. 14. The rocking curve FWHM of the MgO peak increases from 0.36° for STO (top plots) to 0.49°

for LSAT (middle plots) to 1.32° for LAO (bottom plots), in accordance with the increasing lattice mismatch.

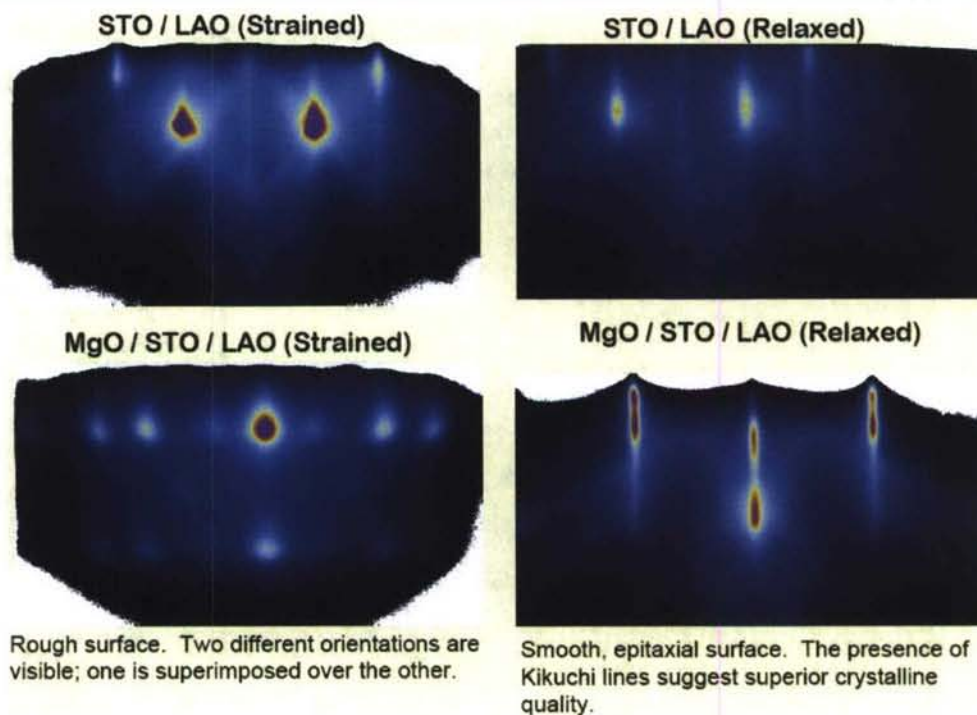


Fig. 16 RHEED patterns of strained / relaxed STO buffer layers on LAO substrates (top left / top right), and MgO epitaxial layers grown on the respective templates. The layer grown on the strained STO / LAO template exhibits a rough surface and two crystal orientations (bottom left), whereas the MgO layer grown on the relaxed STO / LAO template exhibits a smooth surface and high quality single crystal properties.

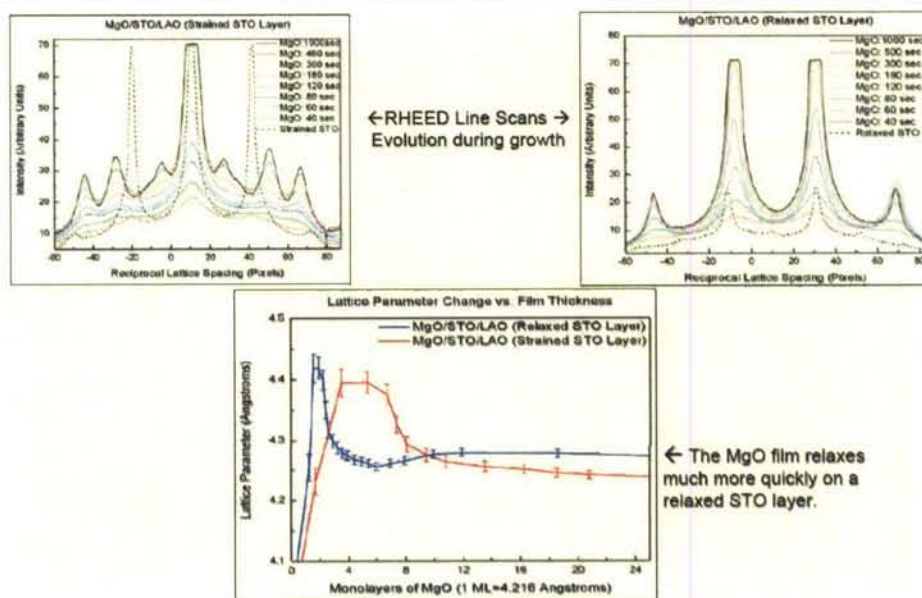


Fig. 17 Evaluation of RHEED line scans as a function of growth time for strained (top left) and relaxed (top right) STO / LAO templates. The plot at the bottom shows the relaxation behavior of the MgO film grown on strained (red curve) and relaxed (blue curve) STO / LAO templates. The MgO layer grown on relaxed STO / LAO exhibits a lattice parameter maximum after approximately two monolayers deposition and a rapid relaxation to bulk values after five monolayers growth. The MgO film grown on the strained template exhibits a maximal lattice parameter peak after approximately 4.5 monolayers growth and relaxation after approximately eight monolayers deposition.

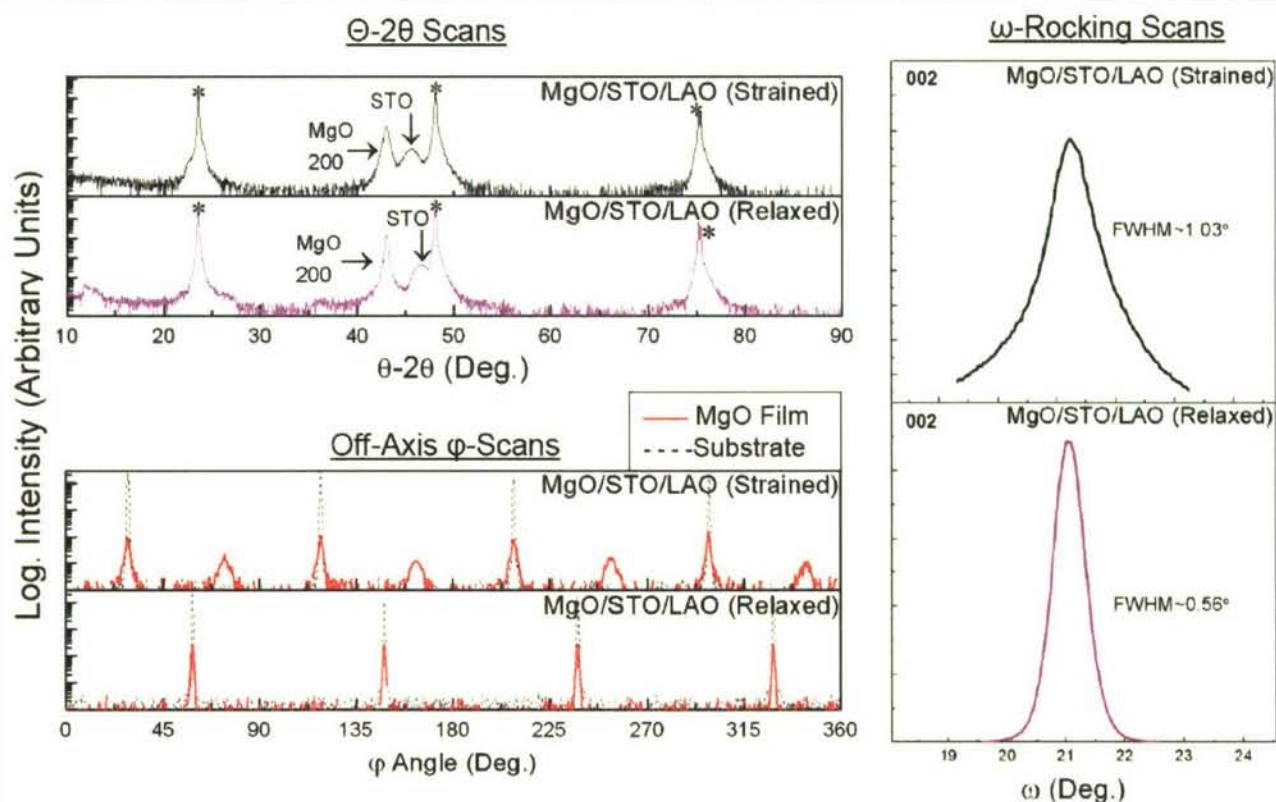


Fig. 18 XRD scans on the MgO films shown in Fig. 16. The FWHM of MgO grown on the strained STO / LAO template is 1.03°, whereas the FWHM of MgO grown on the relaxed STO / LAO template is 0.56°, indicating high film quality.

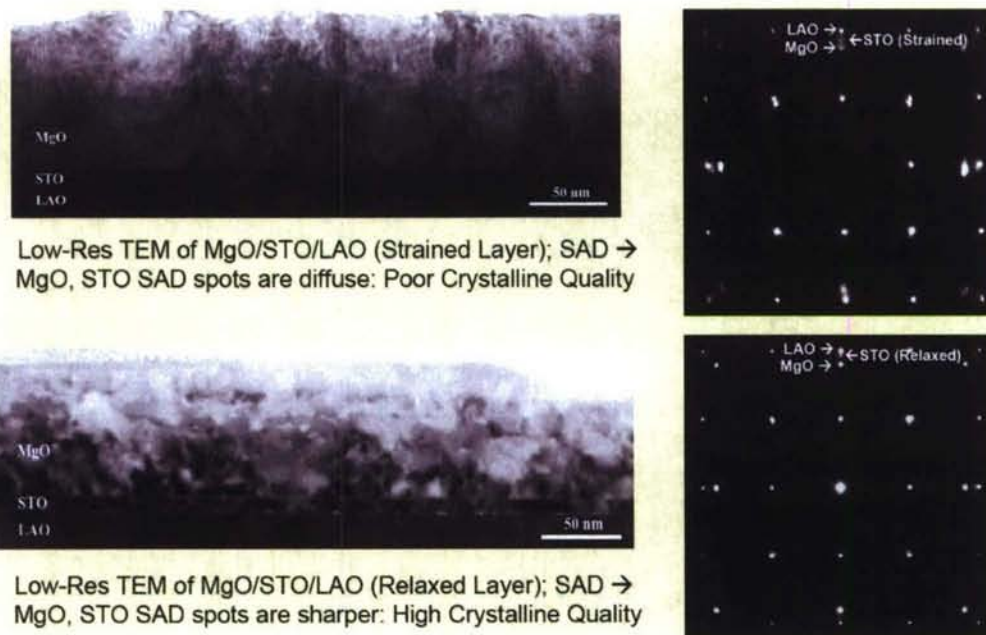


Fig. 19 Low resolution XTEM and SAD (selected area electron diffraction) on MgO epitaxial layer grown on STO buffer layer. The top images show XTEM and SAD on MgO grown on a strained STO buffer layer, the bottom images show XTEM and SAD on MgO grown on a relaxed STO buffer layer. Note the increases contrast in the TEM image on MgO grown on the relaxed STO buffer.

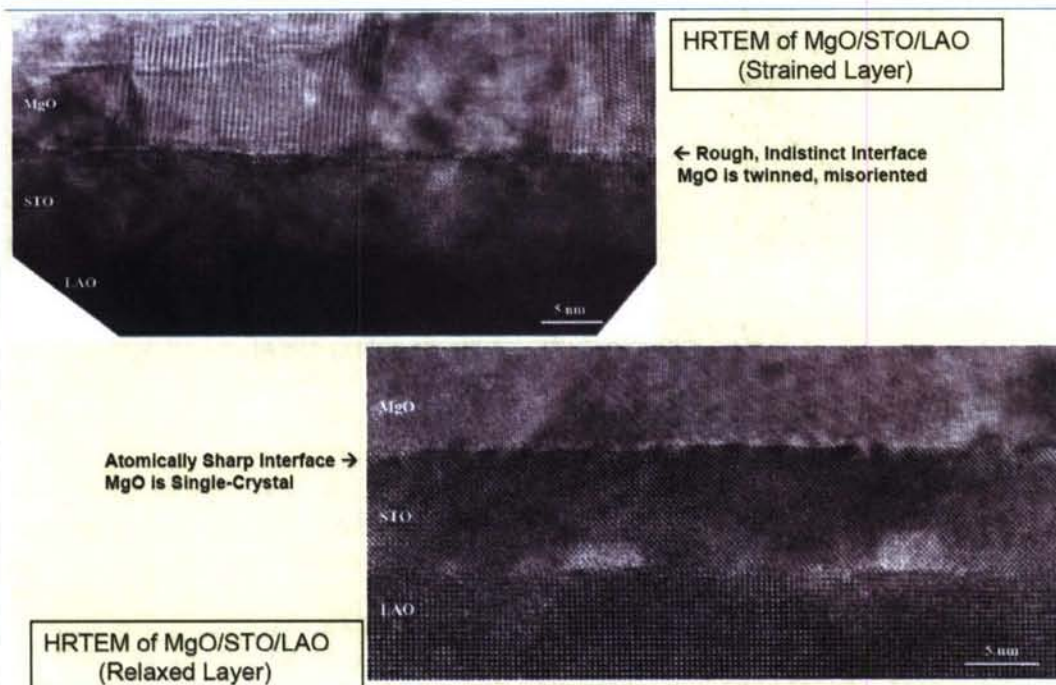


Fig. 20 Comparison of high resolution XTEM on MgO epitaxial layer grown on strained (top) and relaxed (bottom) STO buffer layer. The MgO film grown on the strained STO buffer layer

exhibits columnar oriented grains, whereas the MgO film grown on the relaxed STO buffer layer is continuous showing misfit dislocations.

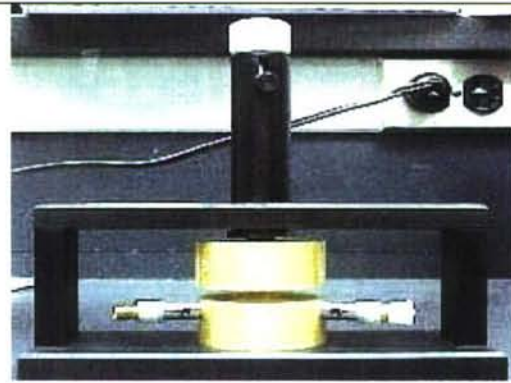
These experiments indicate that the crystal quality of MgO epitaxial layers grown on perovskite substrates / templates shows a strong dependence on the MgO / substrate lattice mismatch. Growth of MgO on STO (7.38% mismatch) resulted in a single crystal MgO film with a ω rocking curve FWHM of 0.36° , on LSAT (8.44% mismatch) in epitaxial MgO growth with misoriented grains with a FWHM of 0.49° , and on LAO (10.1% mismatch) in a polycrystalline MgO film with a FWHM of 1.32° . Growth of MgO on a relaxed STO layer on LAO (7.26% mismatch to MgO) resulted in a single crystal MgO film with a ω rocking curve FWHM of 0.56° , whereas MgO grown on a strained STO layer on LAO (8.21% mismatch to MgO) resulted in an epitaxial MgO film with twinned growth and a ω rocking curve FWHM of 1.03° . From these studies it can be postulated that a MgO / substrate mismatch below 8% yield single crystal MgO growth, and a mismatch in excess of 8% results in growth of twinned or polycrystalline MgO films.

These findings will drive the development of a suitable growth approach for MgO epitaxial layers as buffers between SiC and III-nitride substrates and tunable oxide films. Results from this integration task will be discussed in the next reporting period.

Oxide RF characterization



(a)



(b)

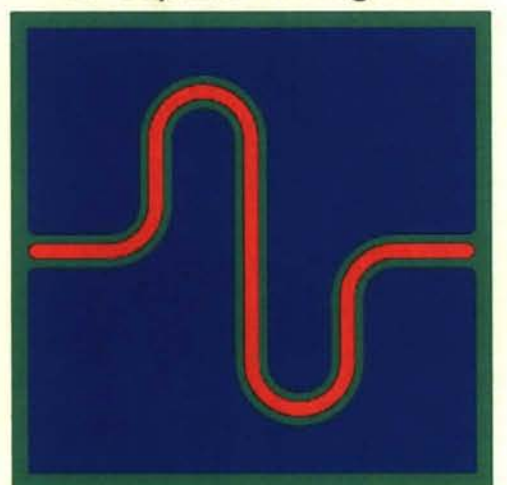
Fig. 21 High frequency test station with network analyzer (a) and split cavity probe fixture (b). The RF test station is used for dielectric characterization of substrate and thin film samples in the frequency range between 1 GHz and 38 GHz.

The microwave characterization of the dielectric properties of SiC substrates was motivated by the necessity to quantify the potential parasitic high frequency losses induced by the SiC substrates when characterizing losses and quality factors in tunable oxide films and devices. The substrate characterization involves measurement of the relative dielectric constant ϵ_r and the loss factor $\tan \delta$, or the quality factor Q , at microwave frequencies, typically 1 – 38 GHz. This characterization will also permit to estimate the losses in tunable oxide devices under their normal operational parameters. A non-contact, non-destructive method for rapid evaluation of SiC substrates was developed to allow for quick turnaround screening of SiC substrates prior to oxide epitaxy. In the course of the evaluation of potential high frequency metrology methods it was desirable to correlate microwave dielectric properties with DC resistivity data derived by IV and eddy current metrology. Data collected under the initial

substrate evaluation task will be used for correlation with future substrate and epitaxial layer RF and DC resistivity and dielectric data. RF measurements were conducted on custom designed split post and split cavity cavities evaluated by a network analyzer. The EOC continues to collaborate with Dr. M. Lanagan (PSU MRL) on the RF metrology task. The Penn State Materials Research Laboratory (MRL) has extensive experience in dielectric materials characterization using prevalently RF network analysis methods. A test station for substrate and thin film evaluation has been set up at MRL permitting split post and split cavity measurements on samples with lateral dimensions between 10mm and 75mm in the frequency range between 1 GHz to 60 GHz (Fig. 21). Split cavity probe stations with resonance frequencies between 1 GHz and 38 GHz have been custom-fabricated. The entire metrology setup was replicated and installed at the EOC to permit fast turnaround on-site evaluation of substrates and oxide thin films and rapid feedback to the crystal growth team.

One benefit of the split cavity test is that the method does not pose any specific dimensional or form factor requirements on substrates and epitaxial layers and that it does not require any time-consuming sample preparation steps, such as contact metallization or mesa structuring. Typically, SiC substrates were subjected to split cavity measurements in the 15 to 20 GHz range, allowing for measurement of the relative dielectric constant between $1 < \epsilon_r < 500$, resolving loss tangents of $10^{-4} < \tan \delta < 10^{-2}$, and quality factors between $50 < Q < 2000$.

RF Coplanar Waveguide



Parameters: Length Width Separation



Fig. 22 Coplanar waveguide structure used for thin film RF characterization. The waveguide and ground plane are structured by laser write lithography.

In addition to the split cavity method, epitaxial layers were characterized using coplanar waveguide measurements. The coplanar waveguide structure is depicted in Fig. 22.

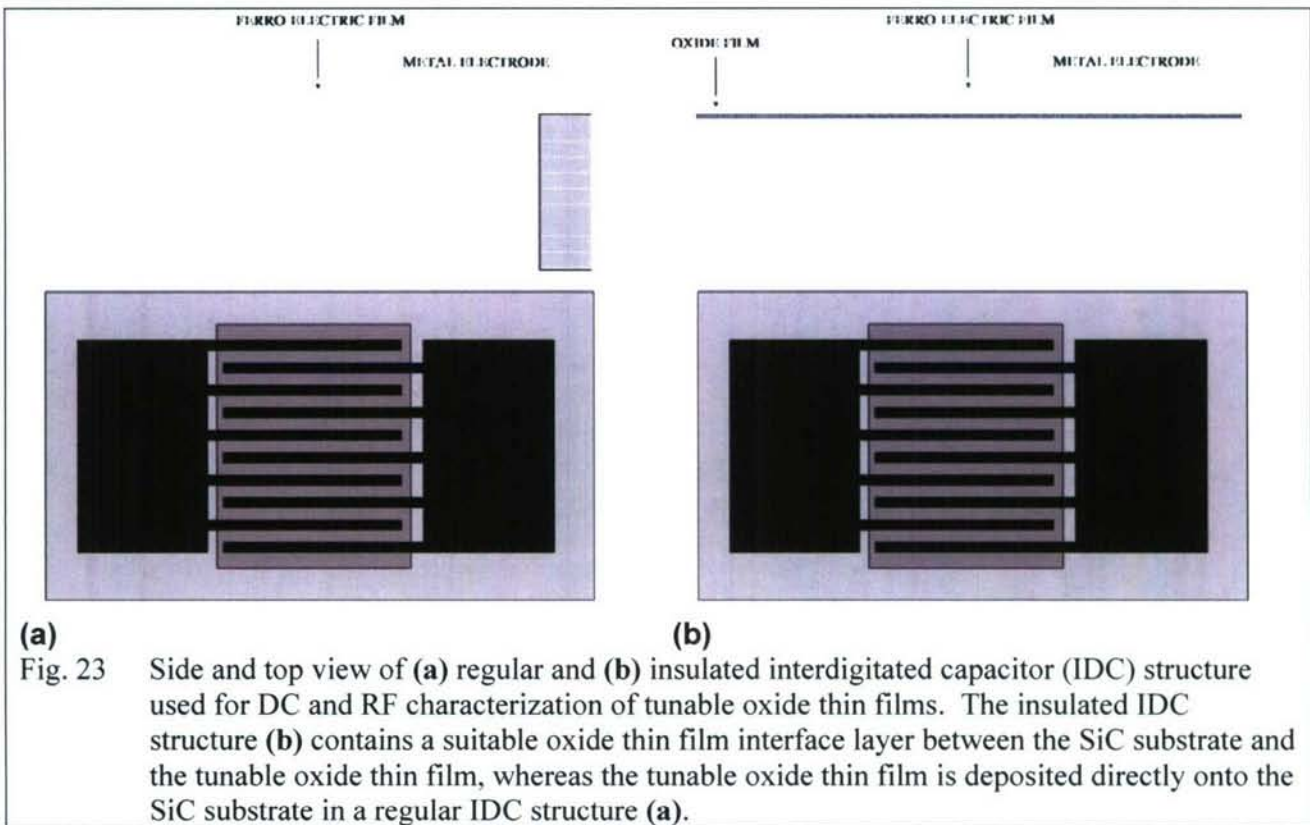
The waveguide structure is created by laser lithography of metal layers on substrates or substrate / epitaxial layer structures. Initial results were obtained on TiO_2 thin films deposited on fused silica SiO_2 substrates. (SiO_2 : $\epsilon_r = 3.78$, TiO_2 : $\epsilon_r = 85$)

This novel approach for evaluation of thin film dielectric properties at microwave frequencies requires simple metallization, simple waveguide fabrication using a laser write on photoresist and a lift off technique. The method requires precise knowledge of the relative dielectric constant ϵ_r , quality factor Q and thickness of the substrate. First measurements were successfully conducted on TiO_2 films on single crystal SiO_2 substrates. The method is proven for the dielectric characterization of thin films with 100nm to 1200nm thickness.

Ferroelectric Varactors

The program targets the fabrication of varactors, i.e. voltage-tunable capacitors as devices that permit evaluation of the quality and suitability of MBE-grown tunable oxide thin films for advanced high power RF systems. Two device layouts are used to produce varactors: Interdigitated capacitors (IDCs) (Fig. 23) and parallel plate capacitors (PPCs) (Fig. 24). Interdigitated capacitors consist of a tunable oxide thin film deposited on a insulating substrate. The oxide film is etched to relieve a mesa structure, and a set of interdigitated electrodes is deposited over top of the oxide film and exposed substrate. Optionally, an additional insulator layer is deposited between the substrate and the tunable oxide thin film to prevent substrate or interface leakage currents (Fig. 23 b). The capacitance, tunability and quality factor of an IDC device are predominantly determined by the oxide layer quality, the contact layer quality, and the geometrical layout of the interdigitated capacitor electrodes.

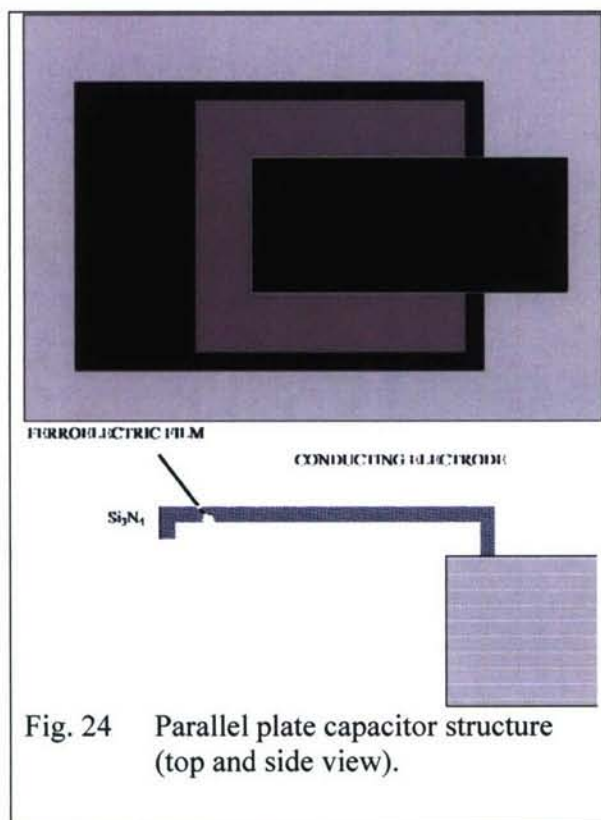
MBE-grown barium strontium titanate (BST) thin films have been used for the fabrication of IDCs using mask sets with finger widths of 1-50 μm , finger lengths of 10-100 μm and finger spacings of 1-20 μm .



(a) **(b)**
 Fig. 23 Side and top view of (a) regular and (b) insulated interdigitated capacitor (IDC) structure used for DC and RF characterization of tunable oxide thin films. The insulated IDC structure (b) contains a suitable oxide thin film interface layer between the SiC substrate and the tunable oxide thin film, whereas the tunable oxide thin film is deposited directly onto the SiC substrate in a regular IDC structure (a).

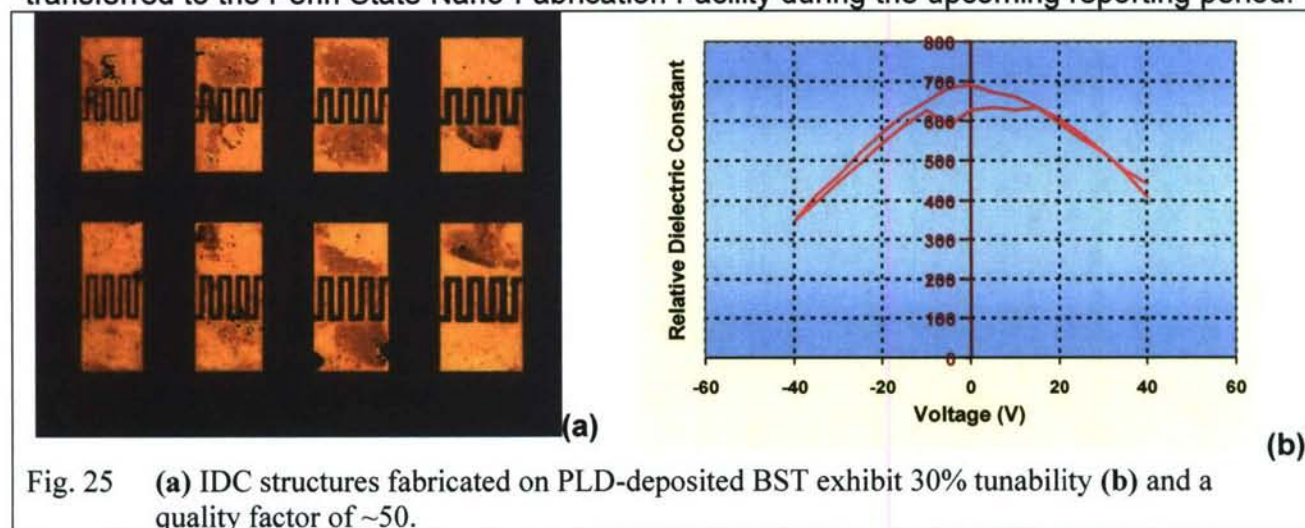
Barium strontium titanate ($\text{Ba}_x\text{Sr}_{1-x}\text{TiO}_3$, BST) was chosen as the active material for the tunable capacitors since ceramic and sputter-deposited BST films have been successfully used for such devices. The material exhibits a large and field dependent dielectric constant, a tunability exceeding 50%, a high breakdown field of 3×10^6 V/cm, low leakage current and a low loss tangent of 0.002 – 0.1 or, respectively, high quality factor of 10 – 500. MBE-grown films offer the promise of improving and customizing the relevant materials parameters by precise control of structural defects, composition and impurities in the BST layers. MBE-grown BST on SiC and III-nitride templates thus far has the drawback of fairly high leakage

currents, an issue that is being addressed by investigation of suitable buffer layers between the substrate / template and the BST film. The goals of this program are to further reduce the loss tangent to 10^{-3} or below, or increase the quality factors beyond 1000, control and customize the SiC / oxide or III-nitride / oxide interface to minimize defect generation, reduce leakage currents and understand and control the interface properties impacting the varactor performance. An investigation of the film stress properties and the film stress evolution will aid the understanding of the tunability mechanism in the films.



The parallel plate capacitor (PPC) structure, depicted in Fig. 24 is an alternative varactor device design. The tunable oxide film is deposited on a conductive bottom electrode, such as strontium ruthenate (Sr_2RuO_4 , SRO), platinum or highly doped SiC or GaN. An insulator film such as Si_3N_4 or SiN_x covers the properly structured tunable oxide film. A metal electrode is deposited on top of the properly structured insulator film. The PPC fabrication requires a series of lithography and etch steps complementing the deposition steps. The advantage of the PPC structure is the utilization of the entire volume of the oxide film underneath the top electrode for tuning, yielding a $\sim 10\times$ lower control voltage and higher device tunability, whereas IDC structures only use a surface-near section of the oxide film exposed between the interlaced finger contacts. Their simpler fabrication process favors IDCs over PPC devices for quick turnaround materials assessment. All tunability and loss data reported here was derived on IDC devices.

The PSU EOC team is working with Dr. Steve Kirchoefer (NRL) to fabricate and characterize interdigitated capacitors on MBE-grown BST epitaxial layers. The fabrication process will be transferred to the Penn State Nano-Fabrication Facility during the upcoming reporting period.



FUTURE WORK (as anticipated at the end of the reporting period):

III-Nitrides

- Establish solid HEMT epitaxial process / epi layer characterization
- Establish HEMT fabrication process / HEMT characterization
- Evaluate HEMT performance and correlate with growth parameters and stress data
- Evaluate HEMT epitaxy on emerging native nitride substrates

Oxides

- Establish solid BST deposition process / composition characterization and control
- Evaluate BST composition impact on tunability and loss performance
- Establish solid MgO buffer layer process on SiC and III-nitrides
- Evaluate MgO impact on subsequent oxide epitaxial layers

III-Nitride / Oxide Integration

- Demonstrate sequential oxide / III-nitride epitaxy
 - Evaluate impact of process parameters on functionality of oxide / III-nitride devices
 - Evaluate protection strategies for oxide / III-nitride layers during epitaxial process
-

References:

- 1 Canedy C.L. et al., *Structural and dielectric properties of epitaxial $Ba_{1-x}Sr_xTiO_3/Bi_4Ti_3O_{12}/ZrO_2$ heterostructures grown on silicon*, Appl. Phys. Lett. **77**(10) 2000 p1523-5
- 2 Keuls F.W.V. et al., *($YBa_2Cu_3O_{7-d},Au$)/ $SrTiO_3/LaAlO_3$ thin film conductor / ferroelectric coupled microstripline phase shifters for phased array applications*, Appl. Phys. Lett. **71**(21) 1997 p3075-7
- 3 Galt D. et al., *Characterization of a tunable thin film microwave $YBa_2Cu_3O_{7-x}/SrTiO_3$ coplanar capacitor*, Appl. Phys. Lett. **63**(22) 1993 p3078-80
- 4 Abadei S. et al., *Low-frequency and microwave performances of laser-ablated epitaxial $Na_{0.5}K_{0.5}NbO_3$ films on high-resistivity SiO_2/Si substrates*, J. Appl. Phys. **91**(4) 1992 p. 2267-76
- 5 Chang W. et al., *The effect of annealing on the microwave properties of $Ba_{0.5}Sr_{0.5}TiO_3$ thin films*, Appl. Phys. Lett. **74**(7) 1999 p1033-5
- 6 Basceri C. et al., *The dielectric response as a function of temperature and film thickness of fiber-textured $(Ba,Sr)TiO_3$ thin films grown by chemical vapor deposition*, J. Appl. Phys. **82**(5) 1997 p2497-504
- 7 Chen C.L. et al., *Epitaxial ferroelectric $Ba_{0.5}Sr_{0.5}TiO_3$ thin films for room temperature tunable element applications*, Appl. Phys. Lett. **75**(3) 1999 p412-5
- 8 Stoney G.G., Proc. Roy. Soc. **82A** (553) 1909 p172
- 9 Tompkins R.P., VanMil B.L., Schires E.D., Lee K., Chye Y., Lederman D., Myers T.H., *In-situ Investigation of Surface Stoichiometry During InGaN an GaN Growth by Plasma-Assisted Molecular Beam Epitaxy Using RHEED-TRAXS*, Mater. Res. Soc. Symp. Proc. **892** (2006), 0892-FF04-06.1

RELEVANT PUBLICATIONS AND PRESENTATIONS

Journal Publications:

"Growth, structure, and morphology of TiO₂ films deposited by molecular beam epitaxy in pure ozone ambients", Salvador, P.A.; Fisher, P.; Maksimov, O.; Hui Du; Heydemann, V.D.; Skowronski, M., *Microelectronics Journal*, v 37, n 12, Dec. 2006, p 1493-7

"Effect of nitridation on crystallinity of GaN grown on GaAs by MBE", Maksimov, O.; Fisher, P.; Skowronski, M.; Heydemann, V.D., *Materials Chemistry and Physics*, v 100, n 2-3, 10 Dec. 2006, p 457-9

"Structural properties of SrO thin films grown by molecular beam epitaxy on LaAlO₃ substrates", Maksimov, O.; Heydemann, V.D.; Fisher, P.; Skowronski, M.; Salvador, P.A. Source: *Applied Physics Letters*, v 89, n 26, 25 Dec. 2006, p 262903-1-3

"Structural and optical properties of GaN films grown on GaAs substrates by molecular beam epitaxy"; Maksimov, O.; Gong, Y.; Du, H.; Fisher, P.; Skowronski, M.; Kuskovsky, I.L.; Heydemann, V.D., *Vacuum*, v 80, n 9, 20 June 2006, p 1042-5

"Growth of GaN films on GaAs substrates in an As-free environment", Maksimov, O.; Fisher, P.; Du, H.; Acord, J.D.; Weng, X.; Skowronski, M.; Heydemann, V.D., *Journal of Vacuum Science & Technology B (Microelectronics and Nanometer Structures)*, v 24, n 3, May 2006, p 1671-5

"Molecular Beam Epitaxial Growth and Dielectric Characterization of Ba_{0.6}Sr_{0.4}TiO₃ Films", P. Fisher, M. Skowronski, P. Salvador, M. Snyder, J. Xu, M. Lanagan, O. Maksimov, V.D. Heydemann, *Mat. Res. Soc. Symp Proc* 966 (2007) 0966-T07-23

"Structural Characterization of TiO₂ Films Grown on LaAlO₃, SrTiO₃, (La_{0.18}Sr_{0.82})(Al_{0.59}Ta_{0.41})O₃, and Al₂O₃ Oxide Substrates", X. Weng, E.C. Dickey, J.M. Redwing, P. Fisher, M. Skowronski, P. Salvador, O. Maksimov, V.D. Heydemann, *J Vac Sci Technol B (in review)*

Conference / Workshop Presentations:

WOCSEMMAD 2005, Oral Presentation:

"Multifunctional Oxide Films for RF Applications", Oleg Maksimov, Volker D. Heydemann, Michael Lanagan, Darrell G. Schlom, Joan M. Redwing, C. Patrick Yue, Patrick J. Fisher, Paul A. Salvador, Marek Skowronski
20–23 Feb 2005, Miami FL

WOCSEMMAD 2006, Oral Presentation:

"Molecular Beam Epitaxy of Integrated Multifunctional Oxides on Wide Bandgap Semiconductors for Advanced RF Systems", O. Maksimov, J.B. Smith, D.J. Rearick, V.D. Heydemann, L. Haney, J. Rankinen, M. Lanagan, W.D. Perez, J.D. Acord, D.G. Schlom, J.M. Redwing, P.J. Fisher, P.A. Salvador, M. Skowronski
19–22 Feb 2006, Scottsdale AZ

WOCSEMMAD 2007, Oral Presentation:

"Recent Advances in the Integration of Multifunctional Oxides on Wide Bandgap Semiconductors", M.J. Snyder, O. Maksimov, J.B. Smith, D.J. Rearick, V.D. Heydemann, W.D. Perez, J.D. Acord, J.M. Redwing, M.T. Lanagan, P.J. Fisher, P.A. Salvador, M. Skowronski
18–21 Feb 2007, Savannah GA

MRS Fall 2006, Poster Presentation T-023

"Molecular Beam Epitaxial Growth and Dielectric Characterization of Ba_{0.6}Sr_{0.4}TiO₃ Films", P. Fisher, M. Skowronski, P. Salvador, M. Snyder, J. Xu, M. Lanagan, O. Maksimov, V.D. Heydemann,
27 Nov – 01 Dec 2006, Boston MA

NAMBE 2005, Poster Presentation P-53:

"Growth of GaN films on GaAs substrates in an As-free MBE chamber", O. Maksimov, P. Fisher, H. Du, M. Skowronski, V.D. Heydemann

NAMBE 2006,

Oral Presentation T48:

"Structure characterization of TiO₂ films grown on various oxides substrates", X. Weng, E.C. Dickey, J.M. Redwing, P. Fisher, M. Skowronski, P. Salvador, O. Maksimov, V.D. Heydemann

Oral Presentation T53:

"Exploration of growth and stability conditions within the SrO – TiO₂ system", P. Fisher, O. Maksimov, H. Du, V.D. Heydemann, M. Skowronski, P. Salvador

NAMBE 2007

Oral Presentation:

"Epitaxial growth of rock salt oxides on perovskite substrates", O. Maksimov, P. Fisher, M. Skowronski, P. Salvador, M. Snyder, J. Xu, X. Weng

Oral Presentation:

"Growth and structural characterization of the novel Sr_mTiO_{2+m} series of phases by MBE", P. Fisher, O. Maksimov, M. Snyder, S. Wang, M. Skowronski, P. Salvador

Poster Presentation P37:

"Growth and structural characterization of the novel Sr_mTiO_{2+m} series of phases by MBE", P. Fisher, O. Maksimov, M. Snyder, S. Wang, M. Skowronski, P. Salvador

APS March 2006

Oral Presentation A46.00006:

"Structural and optical properties of GaN films grown on GaAs substrates by molecular beam epitaxy", O. Maksimov, V.D. Heydemann, P. Fisher, H. Du, M. Skowronski, Y. Gong, I. Kuskovsky

APS March 2007

Oral Presentation P20.00012:

"Molecular Beam Epitaxy of MgO on Perovskite Substrates", M. Snyder, J. Xu, P. Fisher, M. Skowronski, P. Salvador, O. Maksimov, V.D. Heydemann

PSU MRI Materials Day 2005, State College PA

Poster Presentation D05

"Overview of Crystal Growth at the Penn State EOC Materials Department", M. Fanton, D. W. Snyder, W. J. Everson, T. E. Bogart, E. Frantz, O. Maksimov, V. D. Heydemann

Poster Presentation G06

"Molecular Beam Epitaxy of Integrated Multifunctional Oxides on Wide Bandgap Semiconductors for Advanced RF Systems - Overview of Current Activities at the Penn State Electro-Optics Center", O. Maksimov, P. Fisher, M. Skowronski, V. D. Heydemann

PSU MRI Materials Day 2006, State College PA

Poster Presentation C09

"Epitaxial Growth of YMnO₃ by Pulsed Laser Deposition", M. Snyder, J. Xu, O. Maksimov, V. D. Heydemann

Poster Presentation I01

"Growth, Characterization and Optimization of III-Nitride and Multifunctional Oxides for Advanced RF Systems", O. Maksimov, J. B. Smith, D. J. Rearick, V. D. Heydemann, L. Haney, J. Rankinen, M. Lanagan, W. D. Perez, J. D. Acord, X. Weng, J. M. Redwing, P. J. Fisher, P. A. Salvador, M. Skowronski

Poster Presentation I04

"Overview of Crystal Growth at the Penn State EOC Materials Department", D. W. Snyder, M. A. Fanton, W. J. Everson, T. E. Bogart, E. Frantz, R. Shanta, O. Maksimov, V. D. Heydemann

Poster Presentation I05

"Overview of EO Materials Fabrication and Characterization Capabilities", W.J. Everson, E. J. Oslosky, R. D. Gamble, G. M. Goda, D. W. Snyder, T. E. Bogart, M. A. Fanton, V. D. Heydemann

PSU MRI Materials Day 2007, State College PA

Poster Presentation D11

"Design and Processing of High Temperature Electronic Devices and Sensors", D. W. Snyder, M. A. Fanton, V. D. Heydemann, J. Robinson, J. Carter, C. Vaughan, J. M. Redwing, J. Flemish, M. T. Lanagan

Poster Presentation E02

"Integration of Multifunctional Oxides and Wide Bandgap Semiconductors for Advanced RF Applications", V. D. Heydemann, O. Maksimov, D. J. Rearick, J. B. Smith, M. J. Snyder, W. D. Perez, J. A. Acord, X. Weng, J. M. Redwing, P. J. Fisher, P. A. Salvador, M. Skowronski, R. L. Haney, A. L. Baker, M. T. Lanagan

Poster Presentation E03

"Molecular Beam Epitaxy and Characterization of MgO, TiO₂, SrTiO₃, BaTiO₃ and BaSrTiO₃ Thin Films", M. J. Snyder, W. D. Perez, J. A. Acord, X. Weng, J. M. Redwing, P. J. Fisher, P. A. Salvador, M. Skowronski, R. L. Haney, A. L. Baker, M. T. Lanagan, O. Maksimov, D. J. Rearick, J. B. Smith, V. D. Heydemann

EMC 2006, Oral Presentation

"Growth of TiO₂ films by reactive molecular beam epitaxy", P. Fisher, H. Du, P. Salvador, M. Skowronski, O. Maksimov, V.D. Heydemann, X. Weng, J. Redwing

ONR Electronic Device Materials Review 2005, Oral Presentation

"Molecular Beam Epitaxy of Integrated Multifunctional Oxides on Wide Bandgap Semiconductors for Advanced RF Systems", O. Maksimov, J.B. Smith, V.D. Heydemann, M.T Lanagan, P.J. Fisher, M. Skowronski

Red Bank NJ, 14 Aug 2005

ONR Electronic Device Materials Review 2006, (electronic submission only)

"Molecular Beam Epitaxy of Integrated Multifunctional Oxides on Wide Bandgap Semiconductors for Advanced RF Systems", O. Maksimov, J.B. Smith, D.J. Rearick, V.D. Heydemann, W.D. Perez, J.M. Redwing, R.L. Haney, M. Lanagan, J.R. Flemish, P.J. Fisher, P.A. Salvador, M. Skowronski

EMMA Review 2006, Oral Presentation, invited

"Molecular Beam Epitaxy of Integrated Multifunctional Oxides on Wide Bandgap Semiconductors for Advanced RF Systems", O. Maksimov, J.B. Smith, D.J. Rearick, V.D. Heydemann, L. Haney, J. Rankinen, M. Lanagan, W.D. Perez, J.D. Acord, D.G. Schlom, J.M. Redwing, P.J. Fisher, P.A. Salvador, M. Skowronski

Annapolis MD, 11 Jul 2006